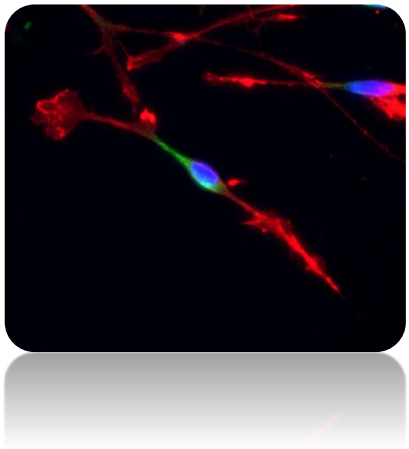


Regulation of developmental myelination in the peripheral nervous system by Rho signalling

Miguel Rafael Gonçalves Morais
Mestrado em Bioquímica
Faculdade de Ciências e Instituto de Ciências Biomédicas Abel Salazar da Universidade do Porto
2018

Orientador
Doutora Ana Seixas, Investigadora
Instituto de Investigação e Inovação em Saúde (i3S); Instituto de Biologia Molecular e Celular (IBMC)

Coorientador
Doutor João Relvas, Investigador Principal
Instituto de Investigação e Inovação em Saúde (i3S); Instituto de Biologia Molecular e Celular (IBMC)

INSTITUTO DE INVESTIGAÇÃO E INOVAÇÃO EM SAÚDE
UNIVERSIDADE DO PORTO

U.PORTO
INSTITUTO DE CIÊNCIAS BIOMÉDICAS ABEL SALAZAR
UNIVERSIDADE DO PORTO

U.PORTO
FACULDADE DE CIÊNCIAS
UNIVERSIDADE DO PORTO

Todas as correções determinadas pelo júri, e só essas, foram efetuadas.

O Presidente do Júri,

Porto, _____/_____/_____

Agradecimentos

Em primeiro lugar gostaria de agradecer aos meus orientadores, Ana Seixas e João Relvas, por me terem dado a oportunidade de realizar este projeto de tese no GCB. Em particular à Ana Seixas agradeço a paciência, disponibilidade, e sobretudo honestidade. No futuro será difícil encontrar um mentor(a) que me permita crescer tanto, quer a nível académico/científico como a nível profissional e de ética de trabalho, como tu fizeste. Qualquer aluno que passe por ti sairá infinitamente mais bem preparado para perseguir uma carreira na ciência. Para além disso (e como é óbvio), todo este trabalho não seria possível sem ti.

Á Camila, ao Pedro e à Raquel, por me integrarem tão bem no GCB, pelo apoio durante os momentos mais difíceis, pelos almoços/lanches/coffee breaks cheios de boa disposição e gargalhadas, pelos inúmeros jantares e passeios e por tantas outras coisas. Este ano teria sido bem mais aborrecido sem a vossa presença. (PS: Ainda temos muitas coisas para riscar da lista, não se esqueçam!)

Aos meus pais, por me terem apoiado incondicionalmente durante toda a minha vida, pela compreensão que demonstraram em particular neste último ano e claro por terem possibilitado a minha formação ao longo destes 5 anos.

À Mariana e à Benedita que me acompanham há muitos anos (quase 20!), pela paciência (que é recíproca!), amizade, companheirismo e essas tretas todas que não vou enumerar. Não tenho espaço e estão fartas de saber. Resumindo, crescemos juntos e eu não seria eu sem vocês. Obrigado!

À Maria Azevedo e à Joana Paes de Faria (Joana, ainda não me esqueci dos enchidos que prometi trazer de Gouveia!) que, na ausência da Ana Seixas, me ajudaram a resolver os problemas que me surgiram, sempre com boa disposição e paciência.

A toda a gente do GCB, por me terem recebido de braços abertos.

A todos os meus familiares e amigos que não nomeei individualmente.

E por último à Faculdade de Ciências (FCUP) e ao Instituto de Ciências Biomédicas Abel Salazar (ICBAS) da Universidade do Porto e ao Instituto de Investigação e Inovação em Saúde (I3S) por me terem acolhido durante a realização deste projeto e durante todo o meu percurso académico.

Abstract

The myelin sheath is a unique multilamellar lipidic membrane that wraps axons and allows for rapid saltatory conduction of action potentials in the vertebrate nervous system. In the early postnatal period, peripheral nervous system axons are myelinated by Schwann cells, which are only capable of forming a single myelin sheath per cell.

In the PNS, large calibre axons are preferably myelinated. Myelination is a multistep process: early in development, large and small axons are grouped in bundles surrounded by immature Schwann cells that extend processes into bundles, recognising and segregating the largest axons in a process called radial sorting. This process is a pre-requisite for correct myelination in the PNS. It relies on major morphogenetic changes in Schwann cells and controlled remodelling of their actin cytoskeleton in order to form plasma membrane protrusions (lamellipodia) that contact and recognise axons. Rho GTPase signalling, in particular, has been shown to be important in Schwann biology during PNS development. Rho GTPases are molecular switches that, among other functions, act as major regulators of cell shape via actin cytoskeleton reorganization. In Schwann cells, the role of Rac1 and Cdc42 in radial sorting has already been demonstrated. Previous studies suggest that Rho signalling is involved in Schwann cell process extension and lamellipodia formation. Recent studies also suggest that RhoA is important for proliferation, migration and differentiation of Schwann cells and myelination. However, the specific role of RhoA in developmental myelination of the PNS, especially *in vivo*, remains unknown.

The aim of this master thesis project was to study the function of the small Rho GTPase RhoA in radial sorting and myelination during PNS development *in vivo* using a conditional knockout mouse model where RhoA is conditionally ablated in myelinating glia (oligodendrocytes and Schwann cells) specifically. Previous findings from our lab include ultrastructural analysis of sciatic nerves sections by electron microscopy, which showed that when expression of RhoA is ablated there is a radial sorting and onset of myelination delay, and a hypomyelination phenotype being present at later stages. In this thesis project, we studied the cell biology of RhoA-deficient SCs and signalling pathways that can be linked to the function of RhoA in PNS myelination. The possible different causes for the observed phenotype(s) were explored. First, we assessed Schwann cell survival in the early postnatal period and found that RhoA appears to be dispensable for this process. Next, we evaluated the possibility that actin cytoskeleton defects are the cause of the radial sorting delay observed. Using an *in vitro* approach, we found that the formation of radial lamellipodia is deficient in the absence of RhoA, but longer processes are being extended by Schwann cells. Subsequent Western blot

analysis of signalling pathways related to actin dynamics revealed that phosphorylation, resulting in inactivation, of the actin severing protein cofilin is increased in RhoA-null Schwann cells. However, expression of other known targets of RhoA, such as the kinases ROCK1 and ROCK2 as well as the actin binding protein profilin, is unchanged suggesting a compensatory mechanism, possibly by RhoC.

Regarding myelination *per se*, Western blot analysis showed a reduction in myelin basic protein levels at postnatal day 25, a timepoint in which myelination is virtually complete, suggesting a delay in myelin production that appears to be independent of Akt signalling, although further experiments are required to confirm this. Using immunofluorescence techniques, we also found that the internode length is reduced. Whether this is attributed to reduction in myelin production or abnormal organization of the nodal/paranodal regions is a question for the future.

Overall, these results support the idea that RhoA has an important role during peripheral nerve development, especially in controlling the morphogenetic changes in Schwann cells that are required for the timely onset of radial sorting and myelination.

Keywords: Peripheral nervous system, sciatic nerve, RhoA, Rho GTPase, Schwann cell, actin cytoskeleton, lamellipodia, myelin.

Resumo

A bainha de mielina é uma membrana lipídica única e multilamelar, que envolve os axónios, permitindo a condução saltatória dos potencias de ação no sistema nervoso dos vertebrados. No sistema nervoso periférico (SNP), os axónios são mielinizados pelas células de Schwann no período pós-natal. As células de Schwann apenas são capazes de formar uma única bainha de mielina por célula.

No SNP axónios de grande calibre são preferencialmente mielinizados. Este é um processo que ocorre em várias etapas: no início do desenvolvimento, axónios de pequeno e grande calibre estão agrupados e rodeados por células de Schwann imaturas que posteriormente estendem processos citoplasmáticos com o objetivo de reconhecer e segregar os axónios de maior calibre – processo denominado *radial sorting*. Este processo é essencial para a mielinização do SNP e para o seu correto desenvolvimento e funcionamento. É dependente de profundas alterações morfogenéticas e da reorganização controlada do citoesqueleto de actina por parte das células de Schwann para que haja a formação de protrusões da membrana citoplasmática (*lamellipodia*) que contactam e segregam os axónios. Estudos anteriores demonstraram que a sinalização por parte de Rho GTPases tem um papel importante na biologia das células de Schwann durante o desenvolvimento do SNP. As Rho GTPases são interruptores moleculares que, para além de outras funções, regulam a morfologia celular via reorganização do citoesqueleto de actina. O papel da Rac1 e da Cdc42 nas células de Schwann durante o radial sorting foi previamente demonstrado. Estudos anteriores sugerem que a sinalização por parte da Rho está envolvida na formação de *lamellipodia* por parte das células de Schwann. Estudos mais recentes também sugerem que a RhoA é importanten para a proliferação, migração e diferenciação das células de Schwann e na mielinização. No entanto, o papel específico da RhoA no desenvolvimento do SNP e mielinização, especialmente *in vivo*, ainda é desconhecido.

O objetivo deste projeto de tese é o de estudar a função da RhoA no *radial sorting* e na mielinização durante o desenvolvimento do SNP. Para isso foi ultilizado um modelo de knockout condicional previamente gerado, em que a RhoA foi condicionalmente deletada nas células gliais mielinizantes (oligodendrócitos e células de Schwann). Antes do início deste projeto, o nosso laboratório realizou análises estruturais de secções de nervo ciático através de microscopia eletrónica que mostraram que na ausência de RhoA existe um atraso no *radial sorting* e no início da mielinização, havendo também um fenótipo de hipomielinização presente em estadios de desenvolvimento mais avançados. Neste projeto de tese foi estudada a biologia celular de células de Schwann deficientes em RhoA e as vias de sinalização que podem estar associadas à sua função

na mielinização do SNP. Foram exploradas as diferentes causas possíveis para o fenótipo observado. Em primeiro lugar foi avaliada a sobrevivência das células de Schwann no período pós-natal. A RhoA aparenta ser dispensável para este processo. De seguida foi avaliada a possibilidade de que defeitos do citoesqueleto de actina são a causa do atraso no *radial sorting*. Usando uma abordagem *in vitro*, foi possível concluir que a formação de *lamellipodia* radiais está afetada na ausência de RhoA, mas também que as células de Schwann estendem processos mais longos. Subsequentemente, a análise por Western blot das vias de sinalização relacionadas com a dinâmica do citoesqueleto de actina revelou que a fosforilação, que resulta em inativação, da *actin severing protein* cofilina está aumentada em células de Schwann que não possuem RhoA. No entanto, a expressão de outros alvos moleculares da RhoA, como por exemplo as cinases ROCK1 e ROCK2, bem com da *actin binding protein* profilina, está inalterada, sugerindo um mecanismo de compensação possivelmente por RhoC.

No que diz respeito à mielinização *per se*, análise por Western blot mostrou uma redução dos níveis de *myelin basic protein* no dia pós-natal 25, um estadio de desenvolvimento em que a mielinização está virtualmente completa. Isto sugere que a produção de mielina sofreu um atraso que aparenta ser independente de sinalização por Akt. No entanto, experiências futuras são necessárias para confirmar esta hipótese. Através de técnicas de imunofluorescência foi possível observar que o comprimento dos *internodes* está reduzido. Se esta observação é atribuída a uma redução na produção de mielina ou a uma organização anormal das regiões nodais/paranodais é uma questão para o futuro.

No geral, estes resultados suportam a ideia de que a RhoA possui um papel importante durante o desenvolvimento do SNP, especialmente no diz respeito ao controlo das alterações morfogenéticas que necessitam de ocorrer nas células de Schwann para o correto início do radial sorting e da mielinização.

Palavras-chave: Sistema nervoso periférico, nervo ciático, RhoA, Rho GTPase célula de Schwann, citoesqueleto de actina, lamellipodia, mielina.

Table of contents

Chapter I: Introduction 1
1.The Peripheral Nervous System 1
1.1. Function and organization 1
1.2. Structure 1
1.2.1. Basic anatomy 1
1.2.2. Cell population 2
1.3. Embryonic development of the PNS 2
1.3.1. Neural crest cells 2
1.3.2. From migrating neural crest cell to Schwann cell precursor 3
1.3.3. From Schwann cell precursor to immature Schwann cell 3
2. The myelin sheath 5
2.1. Origin and function 5
2.2. Formation of the myelin sheath in the PNS - Radial sorting 5
2.2.1. Overview of the molecular mechanisms regulating radial sorting 6
2.3. Onset of myelination 7
2.4. Structure and composition 8
2.5. PNS diseases and regeneration 10
2.5.1. Radial sorting defects 10
2.5.2. Hereditary neuropathies 10
2.5.3. Regeneration after injury 11
3. Rho GTPases and the actin cytoskeleton 12
3.1. Overview of actin dynamics 12
3.2.1. The RhoA subfamily 15
3.3. Rho GTPase signalling in developmental myelination 16
3.3.1. RhoA in SC biology and sciatic nerve development 17
4. Previous findings 19
4.1. Analysis of the early postnatal stage 19
4.2. Analysis of later stages of myelination 20
5. Aims 22
Chapter II: Materials and Methods 23
1. A conditional knockout mouse model for *RhoA* 23
2. Tissue dissection 23
3. Preparation of total protein lysates from fresh tissue 24
4. Western blot analysis 24
4.1. Quantification of WB signal 25
5. Tissue preparation for immunofluorescence (IF) analysis 25

5.1. Frozen sections 25
5.2. Teased fibres 25
6. Primary cultures of Schwann cells 26
7. Immunofluorescence analysis 26
7.1. Immunohistochemistry of teased fibres 26
7.2. TUNEL staining 26
7.3. Immunocytochemistry (ICC) 27
8. Image acquisition and processing 27
9. Statistical analysis 28
Chapter III: Results and discussion 30
1. A Schwann cell-specific knockout mouse model for *RhoA* 30
2. RhoA regulates radial sorting and the onset of myelination 30
2.1. RhoA is dispensable for early post-natal survival of SCs 31
2.2. Process extension is impaired in mutant SCs 31
2.3. Dysregulation of signalling pathways associated with actin dynamics 34
3. Analysis of myelination 37
3.1. Analysis of internode length and myelin protein levels 37
3.2. Signalling pathways that regulate myelin in the PNS 39
Chapter IV: Conclusion and future perspectives 41
Chapter V: References 45

List of Figures

Figure 1 – Neural tube and neural crest development 2
Figure 2 – Schematic representation of the various stages of radial sorting and SC development 5
Figure 3 – Signalling pathways that regulate radial sorting 6
Figure 4 – Signalling pathways that regulate PNS myelination 8
Figure 5 – Schematic representation of an unrolled myelin sheath and its major ultrastructural components 9
Figure 6 – Longitudinal view of a myelinated fibre showing the different regions 9
Figure 7 – Dendritic nucleation model for formation of F-actin networks 12
Figure 8 – Phylogenetic tree of the Ras superfamily of GTPases and respective subfamilies 13
Figure 9 – Different mechanisms for regulation of Rho GTPase activity 14
Figure 10 – Cross-talk between Rac1 and RhoA 15
Figure 11 – Relative levels of active Rac1, Cdc42 and RhoA in sciatic nerves from wild-type mice 16
Figure 12 – Simplified overview of molecular pathways involving Rho signalling and related to the actin cytoskeleton, radial sorting and myelination. 18
Figure 13 – EM images of crossections obtained from P1 and P5 littermates and morphometric analysis 19
Figure 14 – Expression analysis of SC differentiation markers by quantitative real-time PCR in P1 sciatic nerves 20
Figure 15 – EM images of crossections obtained from P15 and P25 littermates and morphometric analysis 20
Figure 16 – Myelinating cell-specific ablation of RhoA using the Cre-Lox system 23
Figure 17 – ICC and Western blot analysis of RhoA levels 30
Figure 18 – TUNEL analysis of P5 sciatic nerve crossections 31
Figure 19 – Process extension is impaired in RhoA cKO SCs. Pull-down analysis of P5 sciatic nerve lysates and quantification of Rac1 and Rac1-GTP levels 33
Figure 20 – Western blot analysis of signalling pathways related to actin dynamics ... 36
Figure 21 – Pull-down analysis of P5 sciatic nerve lysates and quantification of RhoC and RhoC-GTP levels 36
Figure 22 – Internodal length measurements at P25 38
Figure 23 – Western blot analysis of MBP levels at P15 and P25 39
Figure 24 – Western blot analysis of Akt, pAkt 308 and pAkt 473 levels at P15 40

List of Tables

Table 1 – Molecules involved in radial sorting regulation, their function and phenotype when ablated in vivo 7
Table 2 – Protein composition of PNS myelin 10
Table 3 – Interaction between each Rho subtype and some effectors 15
Table 4 – List of primary antibodies used for Western blot and Immunofluorescence . 28
Table 5 – List of secondary antibodies and molecular probes used for Western blot and Immunofluorescence..... 29

List of abbreviations

APES – aminopropyltriethoxysilane

Arp – actin-related protein

BSA – bovine serum albumin

Cdc42 – cell division control protein 42

cKO – conditional knockout

CMT – Charcot-Marie-Tooth

Cnp – 3'-phosphodiesterase

CNS – central nervous system

Cre – causes recombination

DAPI – 4′,6-diamidino-2-phenylindole

DMEM – Dulbecco's modified Eagle's medium

DRG – dorsal root ganglia

DTT – dithiothreitol

ECM – extracellular matrix

EDTA – ethylenediaminetetraacetic acid

EM – electron microscopy

ERM – ezrin, radizin and moesin

Fak – focal adhesion kinase

FCS – fetal calf serum

GAP – GTPase activating protein

GDI – guanine nucleotide dissociation inhibitors

GEF – guanine nucleotide exchange factor

HBSS – Hanks' balanced salt solution

HRP – horseradish peroxidase

ICC – immunocytochemistry

IF – immunofluorescence

ILK – integrin-linked kinase

imSC – immature Schwann cell

IPP – ILK-PINCH-PARVIN

Jab1 – Jun activating binding protein 1

JNK – c-Jun N-terminal kinase

LIMK – LIM kinase

MAPK – mitogen-activated protein kinase

MBP – myelin basic protein

MCD1A – Merosin deficient congenital muscular dystrophy

MEM – minimum essential medium

MLC – myosin light chain

MP – microtubule protecting

NCC – neural crest cell

NRG1 – neuregulin 1

N-WASP – neural Wiskott-Aldrich syndrome protein

P0/MPZ – myelin protein zero

PAK – p21-activated kinase

PBS – phosphate buffered saline

PCR – polymerase chain reaction

PDL – poly-D-lysine

PFA – paraformaldehyde

PNS – peripheral nervous system

Rac1 – Ras-related C3 botulinum toxin substrate 1

Rho – Ras homolog

RIPA – radioimmunoprecipitation assay

ROCK – Rho-associated protein kinase

SC – Schwann cell

SCP – Schwann cell precursor

SDS-PAGE – sodium dodecyl sulfate-polyacrylamide gel electrophoresis

SEM – standard error of the mean

SGC – satellite glial cell

SSC – saline-sodium citrate

TBS – Tris buffered saline

TBS-T – Tris buffered saline with 0,1% Tween 20

TEM – transmission electron microscopy

TUNEL – terminal deoxynucleotidyl transferase dUTP nick end labelling

VEGF – vascular endothelial growth factor

WAVE – WASP family Verprolin-homologous

Chapter I: Introduction

1.The Peripheral Nervous System

1.1. Function and organization

The nervous system maintains organism homeostasis by coordinating essential body functions while also being responsible for higher cognitive abilities, such as learning, memory and social behaviour. This is accomplished by action potentials and chemical signals that are generated by neurons and can be transmitted between them through synapses. The main function of the nervous system is to generate, process and distribute these complex signals throughout the organism.

The nervous system can be structurally divided into central nervous system (CNS) comprised by the brain, spinal cord and the optic nerve, and the peripheral nervous system (PNS). The PNS generates the nerve impulse through specialized sensory receptors, transports the signal to the CNS and communicates the central response to the respective effectors in the periphery. It can be divided according to sensory (afferent) and motor (efferent) functions. The efferent division is comprised of a somatic component (SNS - somatic nervous system) which is consciously controlled and conveys output from the CNS to skeletal muscles, and an autonomic component (ANS - autonomic nervous system) which carries the output signal from the CNS to cardiac and smooth muscle and glands. The ANS can also be divided into two components, the sympathetic and parasympathetic nervous system that have opposite actions over the effectors, plus the enteric nervous system (Tortora et al. 2016).

1.2. Structure

1.2.1. Basic anatomy

The vertebrate PNS includes cranial and spinal nerves, the enteric plexuses in the small intestine, and sensory receptors. There are 2 pairs of cranial nerves that originate from the brain, while the other 10 pairs originate from the brainstem (Catala et al. 2013). Spinal nerves are formed by a dorsal and a ventral (efferent) root that emerge from the spinal cord through notches between vertebrae. The 31 pairs of spinal nerves can be categorized according to the region of the spine from which they originate (cervical, thoracic, lumbar, sacral and coccygeal). The sciatic nerve, of particular interest for this work, originates in the sacral region at the bottom of the spine (L4-S3) and is composed by the tibial and fibular nerves surrounded by a common sheath of connective tissue.

1.2.2. Cell population

In general, neural tissues are composed of several types of cellular elements. Neurons are the communicating cells, while glial cells have a wide range of functions, such as maintenance of the extracellular milieu, formation and maintenance of the blood-brain barrier in the CNS and myelination. Glia also plays a role in regulating synaptic transmission, formation of synaptic contacts (Barker et al. 2008; Wu et al. 2015) and in inflammatory, pain and neurological disorders (Giaume et al. 2007).

PNS neurons can be classified according to their structure, depending on the number of processes that extend from their cell body, or functionally classified according to the direction of the nerve impulse they convey: sensory neurons convey sensory input into the CNS, motor neurons from the CNS to effectors (Tortora et al. 2016).

The glial cell population in the PNS is comprised of satellite glial cells (SGCs) and Schwann cells (SCs). SGCs are closely associated with neurons in dorsal root ganglia (DRG), surrounding their cell bodies, providing structural support and regulating exchanges between them and interstitial fluid (Hanani 2005). SCs are responsible for myelination of axons in the PNS and also exhibit some phagocytic capabilities.

1.3. Embryonic development of the PNS

1.3.1. Neural crest cells

In the early embryonic development of vertebrates, the primordium of the nervous system, the neural plate, originates from the ectoderm in a process called neural induction. Later, neurulation occurs, and the neural plate gives rise to the neural tube that will originate the CNS and motor neurons of the PNS (*Figure 1*). Briefly, the neural tube suffers a ventro-dorsal polarization induced by the surrounding tissues (dorsal – notochord; ventral – surface ectoderm) that secrete morphogens, which act in a concentration-dependent way to switch on genes that encode for lineage-specific transcription factors. (Echelard et al. 1993).

In contrast, sensory neurons and glia of the PNS arise from the neural crest cells (NCC), a multipotent stem cell population that also gives rise to the enteric PNS, endocrine cells of the adrenal gland, pigment cells, craniofacial bones and cartilage and cardiac structures (Mayor et al. 2013). NCCs originate from the interface between the surface ectoderm and the neuroectoderm, and subsequently undergo epithelial-mesenchymal transition and

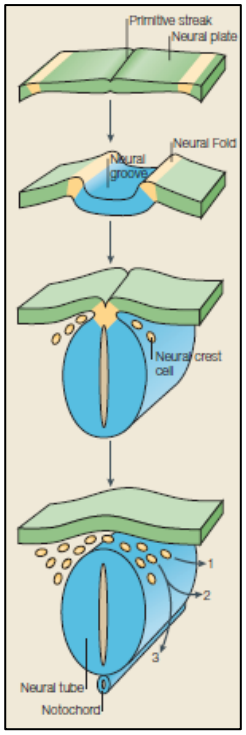


Figure 1 – Neural tube and neural crest development. Trunk NCCs can migrate through lateral (1) or ventral (2 and 3) directions. Adapted from (Jessen et al. 2005).

migrate into surrounding tissues (Theveneau et al. 2012). At first this migration occurs as a continuous wave, but later separates into distinct routes that determine the fate of NCCs. PNS sensory neurons and glia derive from trunk NCCs that migrate through the ventral pathway (*Figure 1*) (Weston 1963; Jessen et al. 2005).

1.3.2. From migrating neural crest cell to Schwann cell precursor

The generation of the different non-neuronal cell populations of the PNS (gliogenesis) begins when newly formed DRG neurons upregulate *Delta1* that acts in neighbouring *Notch*-expressing NCCs, inhibiting neurogenesis and promoting proliferation and gliogenesis (Morrison et al. 2000; Wakamatsu et al. 2000). The first stage of embryonic SC development is the generation of Schwann cell precursors (SCP) (*Figure 2*), which in mice happens from embryonic day (E)12 to E13 (Jessen et al. 1994). The main differences between this stage and migrating NCCs is that SCP are associated with axons, depend on them for survival and are strongly biased towards SC generation (Jessen et al. 2005). In spinal dorsal and ventral roots, SCs have a slightly different origin: boundary cap cells are a transient and multipotent subpopulation of NCC that form an indispensable barrier between the PNS and the CNS and also give rise to nociceptive neurons in DRG, satellite glia and Schwann cells (Aquino et al. 2006; Maro et al. 2004).

Axon-dependent survival is important at this stage to match the number of axons and SCPs, as the establishment of a 1:1 ratio is a pre-requisite for myelination. Axonal neuregulin 1 (NRG1) inhibits the development of neurons (Shah et al. 1994) and it is an essential survival factor for SCPs *in vivo* (Marchionni et al. 1993), in particular the type III isoform (Wolpowitz et al. 2000). The transcription factor Sox10 (sex determining region Y box 10) is also essential for peripheral glia development as evidenced by the lack of both SCs and SGCs in mice that carry a mutation in *Sox10*. In fact, Sox10 is required for appropriate *ErbB3* expression in neural crest cells (Britsch et al. 2001). ErbB3 belongs to the family of epidermal growth factor receptor tyrosine kinases that bind neuregulins and requires ErbB2 as a coreceptor (Garratt et al. 2000). *Sox10* is expressed in NCCs when they dissociate from the neural tube, is maintained during migration and is present in the glial lineage (Kuhlbrodt et al. 1998). Additionally, studies in zebrafish have shown that Nrg1 type III signalling through ErbB2 receptor is essential for SCPs to migrate along neurons during development (Perlin et al. 2011).

1.3.3. From Schwann cell precursor to immature Schwann cell

The development from SCP to immature Schwann (imSC) cell occurs between E13 and E15. This transition stage is marked by loss of migratory ability, formation of basal lamina and the switch between axon-dependent survival to autocrine survival. At this

stage of development, small and large axons are grouped in bundles by multiple imSCs that organize a common basal lamina around them (Jessen et al. 2005). Although the molecular mechanisms behind this are not fully understood, axonal Notch signalling appears to be important. Loss of Notch1 *in vivo* inhibits imSC formation and decreases SCP proliferation, while its overactivation has the opposite effect (Woodhoo et al. 2009).

During this stage of development, SCPs and axons are the only cellular components of peripheral nerves. Blood vessels and the perineurial/epineurial sheaths that surround mature nerves are not yet developed and imSCs play an essential role in their differentiation, since they secrete vascular endothelial growth factor (VEGF) (Mukouyama et al. 2005) and Dhh (Parmantier et al. 1999).

The subsequent developmental stages of Schwann cell differentiation, as well as the role of imSCs in myelination are discussed in the next section.

2. The myelin sheath

2.1. Origin and function

The myelin sheath is a multilamellar layer of electrically insulating, specialized plasma membrane of myelinating glial cells (CNS – oligodendrocytes; PNS – Schwann cells) that surrounds axons, allowing for rapid saltatory conduction of the nerve impulse. This not only increases the speed but also the efficiency of impulse transmission. Myelin is also important in shaping the axon's membrane organization as for example ion channels are restricted to specific areas known as nodes of Ranvier (Trapp et al. 2004). This constitutes an enormous evolutionary advantage as it allows for the development of larger body structures and facilitates both predatory and escape behaviours. It is believed that the appearance of the myelin sheath and the hinged jaw coincide (Zalc et al. 2008).

2.2. Formation of the myelin sheath in the PNS - Radial sorting

In the PNS, before the myelination process *per se* occurs, imSCs need to recognise and segregate larger axons to the periphery of mixed calibre axon bundles, since axons with more than 1µm in diameter preferably get myelinated (Webster et al. 1973). This multistep and morphogenetic process is called radial sorting and begins perinatally, continuing until around postnatal day (P) 10 in mice (*Figure 2*). In short, radial sorting begins with the formation of mixed calibre axon bundles surrounded by three to eight imSCs that organize a basal lamina (stage 1) and extend processes into the bundles (stage 2), recognising (stage 3) and segregating larger axons to the periphery (stage 4). During the last stage (stage 5), and in order to acquire a 1:1 relationship with axons, imSCs proliferate and differentiate into pro-myelinating SCs and lastly defasciculate,

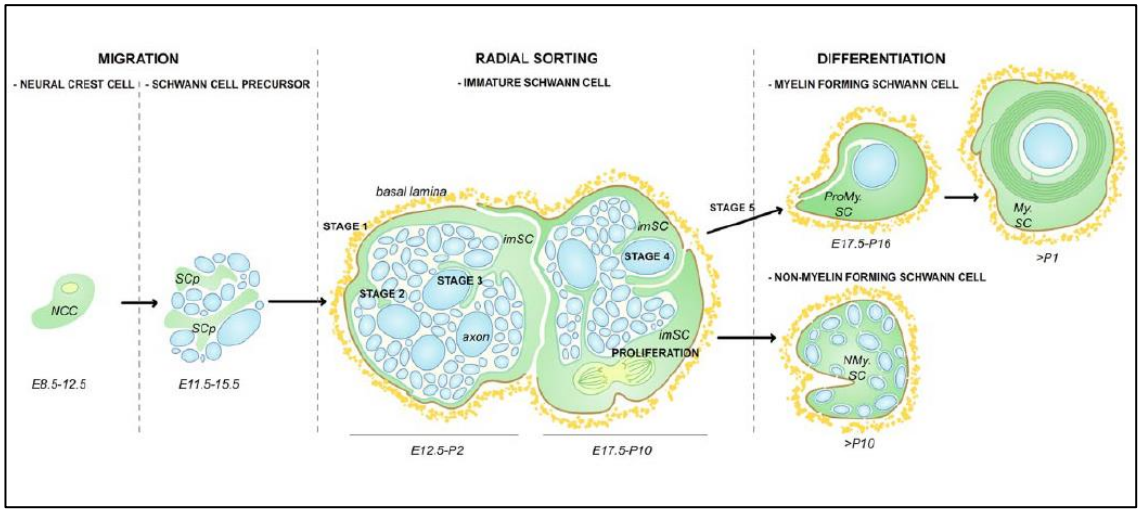


Figure 2 – Schematic representation of the various stages of radial sorting and SC development. Adapted from (Feltri et al. 2016).

forming their own basal lamina. Subsequently, SCs align with the axon and become polarized, with the outer mesaxon (the outer cell membrane that is in contact with the basal lamina) anchored to the basal lamina and the inner mesaxon in contact with the axon membrane. Later in the postnatal period, the remaining imSCs that are in contact with small calibre axons differentiate into non-myelinating SCs to form Remak bundles (Feltri et al. 2016).

2.2.1. Overview of the molecular mechanisms regulating radial sorting

Radial sorting is a limiting step in myelination. The spatial-temporal control of the different stages of radial sorting depends on multiple signalling pathways (*Table 1*) that are involved in regulating SC polarization, proliferation and morphology and often involve rearrangements of the actin cytoskeleton (*Figure 3*). Several recent studies indicate that these signalling pathways are controlled in response to ECM (extracellular matrix) components and axonal signals. Receptors like Integrin α6/β1 and dystroglycan mediate ECM-derived signalling, activating intracellular downstream targets that control SC proliferation (Fak-focal adhesion kinase; Cdc42-cell division control protein 42; Jab1- Jun activating binding protein), polarization and actin cytoskeleton dynamics to form cellular protrusions (Rho- Ras homolog; Rac1- Ras-related C3 botulinum toxin substrate 1; N-Wasp, Profilin) (Monk et al. 2015). Axon-derived signals also play a role through Wnt and respondins paracrine signalling (Grigoryan et al. 2013). Regarding gene expression, deletion of Dicer, an enzyme that generates micro-RNAs, in SCs delays radial sorting and arrests myelination suggesting its importance for the control of the gene expression program (Pereira et al. 2010).

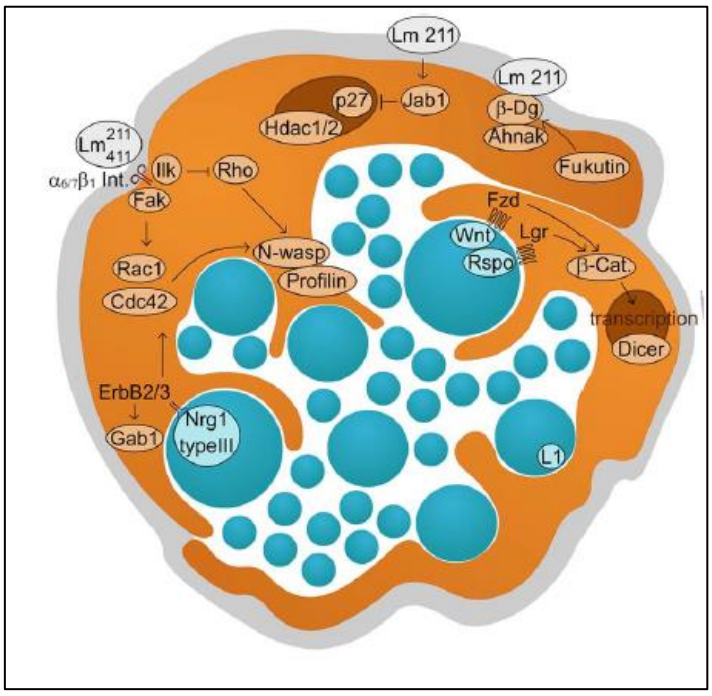


Figure 3 – Signalling pathways that regulate radial sorting. ECM components like Laminins (Lm) 211 and 411 activate intracellular pathways through Integrin (Int.) and dystroglycan (Dg) receptors in SCs. These pathways regulate SC polarization, proliferation (Fak, Cdc42, Jab1) and actin cytoskeleton dynamics (Rho, Rac1, N-Wasp, Profilin). Adapted from (Monk et al. 2015).

Table 1 – Molecules involved in radial sorting regulation, their function and phenotype when ablated *in vivo*.

Protein	Function	Phenotype	Reference (s)
Integrin β1	Adhesion molecule	Early radial sorting arrest	(Feltri et al. 2002)
Integrin α6	Adhesion molecule	Late radial sorting arrest	(Pellegatta et al. 2013)
ILK	Signalling molecule	Early radial sorting arrest	(Pereira et al. 2009)
Fak	Signalling molecule	Early radial sorting arrest	(Grove et al. 2007)
Dystroglycan	Adhesion molecule	Late radial sorting arrest	(Berti et al. 2011)
Laminin α2	ECM	Early radial sorting arrest	(Yang et al. 2005)
Laminin α4	ECM	Early radial sorting arrest	(Wallquist et al. 2005; Yang et al. 2005)
Laminin γ1	ECM	Early radial sorting arrest	(Chen et al. 2003)
Collagen XV	ECM	Polyaxonal myelination	(Rasi et al. 2010)
Rac1	Rho GTPase	Early radial sorting delay	(Benninger et al. 2007; Nodari et al. 2007)
Cdc42	Rho GTPase	Late radial sorting arrest	(Benninger et al. 2007)
N-WASP	Actin polymerization	Early radial sorting delay	(Novak et al. 2011)
Profilin 1	Actin polymerization	Early radial sorting delay	(Montani et al. 2014)

2.3. Onset of myelination

The transition from pro-myelinating SC to myelinating SC begins at around P1, with myelination peaking at P15 (*Figure 2*). It is axon dependent and mainly axons with a diameter above 1µm are myelinated (Friede Reinhard 1972). There is a direct correlation between levels of NRG1 type III in axons and their potential to be myelinated (Taveggia et al. 2005), and myelin sheath thickness (Michailov et al. 2004). Other pathways include the PI-3 kinase/AKT/mTOR (Goebbels et al. 2010), and mitogen-activated protein kinase (MAPK) (Newbern et al. 2011), as well as cAMP signalling and Ca^{2+}/calcineurin activation (Kao et al. 2009) (*Figure 4*). In general, the regulation of these signalling pathways leads to activation of transcription factors that upregulate expression of the main myelin components. For example, Krox-20 is a master transcriptional regulator of pro-myelinating SCs, since in its absence axons are not myelinated as SCs are arrested at the pro-myelinating stage (Topilko et al. 1994). Also, Krox-20 is required for myelin maintenance as its tamoxifen-induced deletion in adult peripheral nerves results in demyelination and dedifferentiation of SCs (Decker et al. 2006). The POU domain transcription factor Oct-6 is expressed in pro-myelinating SC, especially during the

transition to myelinating SC and is downregulated when myelination begins (Arroyo et al. 1998). It is important for myelination to occur since it regulates Krox-20 expression (Ghislain et al. 2002) and in Oct-6 null mice this expression, as well as myelination, occurs after a developmental delay of about two weeks (Jaegle et al. 1996). Sox10 is also important during this stage, as it has been reported to act synergistically with Oct-6 to promote Krox-20 expression (Jagalur et al. 2011).

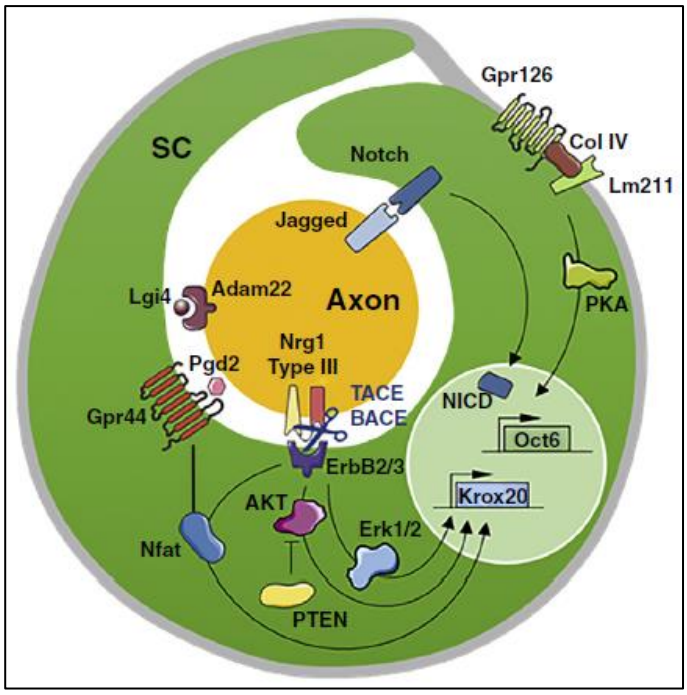


Figure 4 – Signalling pathways that regulate PNS myelination. Axonal NRG1 type III activates signalling pathways that ultimately lead to transcription of myelin genes. Other pathways depicted are the activation of cAMP signalling by Gpr126, Jagged/Notch signalling and Lgi 4 binding to ADAM22. Adapted from (Taveggia 2016).

2.4. Structure and composition

The initial light microscopy observations by Ramon y Cajal described the myelin sheath and SCs as being separate entities. Only with the arrival of transmission electron microscopy (TEM) the myelin sheath ultrastructure began to be unveiled. The initial description of myelin as a spiralled extension of the SC plasma membrane in the PNS was published in 1954 (Ben Geren 1954).

The myelin internode, which corresponds to the myelin segments between two unmyelinated regions (nodes of Ranvier), can be divided in compact and noncompact myelin. Most of the internode is comprised by compact myelin while noncompact myelin allows cytoplasmic continuity between SCs and regions of the internode (*Figure 5*). Schmidt-Lanterman incisures are cytoplasmic channels that cross compact myelin, connecting inner and outer areas of the internode and containing SC cytoplasm. The lateral loops present in the paranodal region are of extreme importance for myelin-axon adhesion, forming septate-like junctions (Trapp et al. 2004). At the node region (*Figure 6*), SCs contact axons through microvilli and regulate the concentration of the various molecules present in this region.

Nodes of Ranvier are enriched in voltage-gated sodium channels, K^+ channels that regulate neuronal excitability and scaffolding proteins like ankyrin G and βIV spectrin that cluster the channels during development and link them to the cytoskeleton (Rasband et al. 2015).

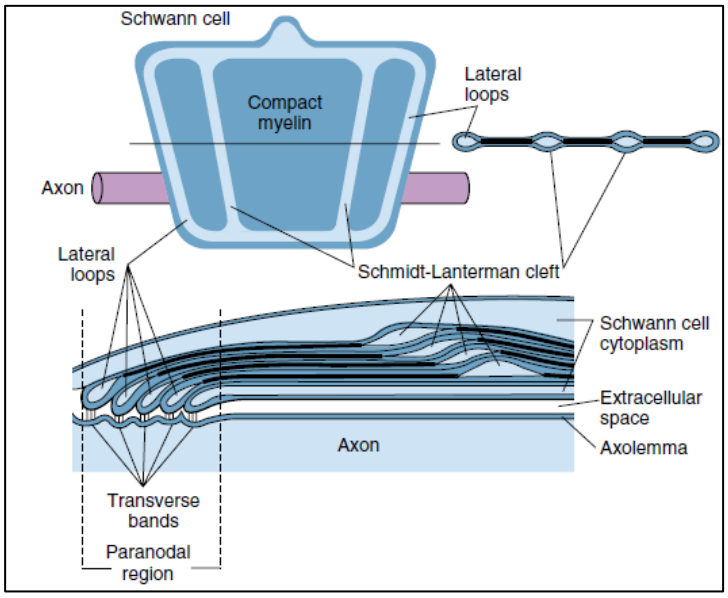


Figure 5 – Schematic representation of an unrolled myelin sheath and its major ultrastructural components. Adapted from (Rasband et al. 2012).

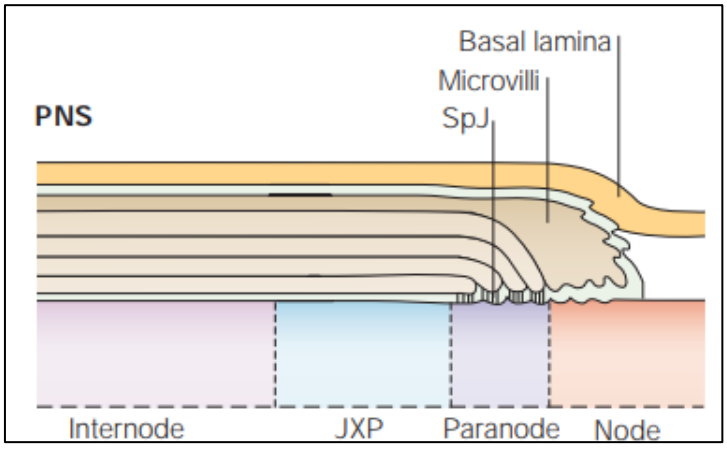


Figure 6 – Longitudinal view of a myelinated fibre showing the different regions. JXP- juxtaparanode; SpJ- Septate-like junction. Adapted from (Poliak et al. 2003).

The myelin sheath has a 70 to 80% composition in lipids and 20 to 30% in proteins (*Table 2*). This high lipid content and their particular characteristics are responsible for the electrically insulating properties of myelin, although there are no myelin-specific lipids. While the relative quantitative distributions of lipid subclasses seems to vary among species (Norton et al. 1984), cholesterol is believed to be one of the most important components (Saher et al. 2005).

The glycoprotein myelin protein zero (P0, MPZ) is the major structural component of PNS myelin and is important for adhesion of the extracellular and cytoplasmic surfaces of myelin sheaths. Both mRNA and protein levels of P0 can be detected prior to myelination in SCs, from the SCP stage onwards, although there is a significant increase in its levels during active myelination (Lee et al. 1997). This suggests P0 has a role in SC differentiation.

Myelin basic protein (MBP) is the second most abundant myelin protein in the PNS. In rodents, this protein exists in multiple isoforms that are produced by alternative splicing of a single gene (Roach et al. 1985). It is localized at the cytoplasmic surface of compact myelin and it is believed to play an important role, together with P0, in maintaining the

major dense line and in compaction of the myelin sheath (Garbay et al. 2000). However, MBP is not essential for PNS myelin formation. The Shiverer mouse, which carries an autosomal recessive mutation that results in loss of MBP expression, has a hypomyelinated CNS but a relatively normal PNS (Readhead et al. 1990).

Table 2 – Protein composition of PNS myelin. Adapted from (Garbay et al. 2000).

	Abundance in myelin (% of total myelin proteins)	Molecular mass (mature protein) (kDa)
Glycoproteins		
P0	50–70%	28
PMP22	2–5%	22
MAG	1%	100
Periaxin	5%	170
E-cadherin	< 0.5	130
Basic proteins		
MBP	5-15%	14–21.5
P2	1–10%	14.8
Other proteins		
CNP	< 0.5%	46/48
PLP/DM20	< 0.5%	30/25
Cx32	< 0.5%	32

2.5. PNS diseases and regeneration

The importance of myelin for the proper function of the PNS is highlighted by the existence of various diseases in which defective myelin is the major cause. This can be due to failure in correctly assembling or maintaining the myelin sheath (dysmyelinating diseases), while in demyelinating diseases the pre-existing myelin is damaged or lost, leading to axonal degeneration (Love 2006).

2.5.1. Radial sorting defects

In humans, radial sorting defects lead to peripheral dysmyelinating neuropathies characterized by bundles of unsorted axons, irregular myelination, short internodes and atypical nodes of Ranvier. For example, loss of function of the *LAMA2* gene that encodes the α2 chain of Laminin 211, a major constituent of the basal lamina of SCs, results in Merosin deficient Congenital Muscular Dystrophy (MCD1A) a subtype of congenital muscular dystrophy (Feltri et al. 2016).

2.5.2. Hereditary neuropathies

Charcot-Marie-Tooth (CMT) is the most common inherited neuromuscular condition with a prevalence of 1:2500 (Reilly et al. 2011). It is characterized by weakness and sensory loss that starts at lower limbs and progresses slowly, with distal muscle weakness and wasting. An heterogenous disorder, CMT can be divided in demyelinating (CMT1) and axonal (CMT2) forms based on nerve conduction velocities. Mutations in more than 80 genes have been identified (Rossor et al. 2013). The most common form is CMT1A, caused by a duplication in the short arm of chromosome 17 that contains the peripheral myelin protein 22 (*PMP22*) gene (Raeymaekers et al. 1991). Another relatively common form, CMT1B, is caused by a point mutation in the *MPZ* gene (Hayasaka et al. 1993).

2.5.3. Regeneration after injury

In the PNS, repair after traumatic nerve injury is achieved through regeneration of damaged axons and reinnervation of target tissues. This is accomplished by cooperative cellular and molecular events that provide a permissive environment for axonal regrowth. The process that leads to degeneration of the part of the axon distal to the injury site is called Wallerian degeneration (Stoll et al. 1999). During this process, SCs that surround the original nerve fibre undergo de-differentiation and downregulate myelin associated proteins, such as myelin-associated glycoprotein (Wolpowitz et al.), which inhibit axonal regrowth capacity (Mukhopadhyay et al. 1994; Shen et al. 1998). This process is transcriptionally controlled by the expression of the transcription factor c-jun in SCs (Jessen et al. 2016). These SCs remain surrounded by a basal lamina and begin to proliferate, forming Bunger bands that allow the establishment of a permissive environment for axon regrowth (Fawcett et al. 1990). Remyelination takes place when SCs in Bunger bands contact re-growing axons, in a process that is thought to be similar to developmental myelination (Chen et al. 2007).

3. Rho GTPases and the actin cytoskeleton

3.1. Overview of actin dynamics

In eukaryotes, the cytoskeleton is essential for spatial organization and mechanical properties of cells. In general, in animal cells there are three types of cytoskeletal filaments: intermediate filaments that provide mechanical strength, microtubules that mediate intracellular transport and govern the positioning of organelles, and actin filaments that underlie the plasma membrane, shaping the cell's surface and forming highly dynamic structures essential for cell motility and cell-cell contact. Actin filaments are built from globular monomers called G-actin, that associate with each other to form polymers of F-actin (*Figure 7*). G-actin subunits bind ATP or ADP and incorporation of ATP-actin into a growing filament leads to rapid cleavage of ATP into ADP and inorganic phosphate (Pi). Treadmilling, during which G-actin-ATP monomers are added to the + (or barbed) end and G-actin-ADP monomers shed from the – (or pointed) end, results in the constant recycling of subunits between the filaments and the cytosol. This remarkable turnover rate, driven by the action of various actin-binding proteins, allows for high spatial and temporal flexibility of the actin cytoskeleton (Alberts et al. 2008).

The formation of different types of protrusive structures relies primarily on the formation of cross-linked F-actin networks near the plasma membrane. Filament assembly and elongation results from the action of nucleation proteins such as the Arp2/3 complex (actin-related proteins), which can build a branched network from individual F-actin

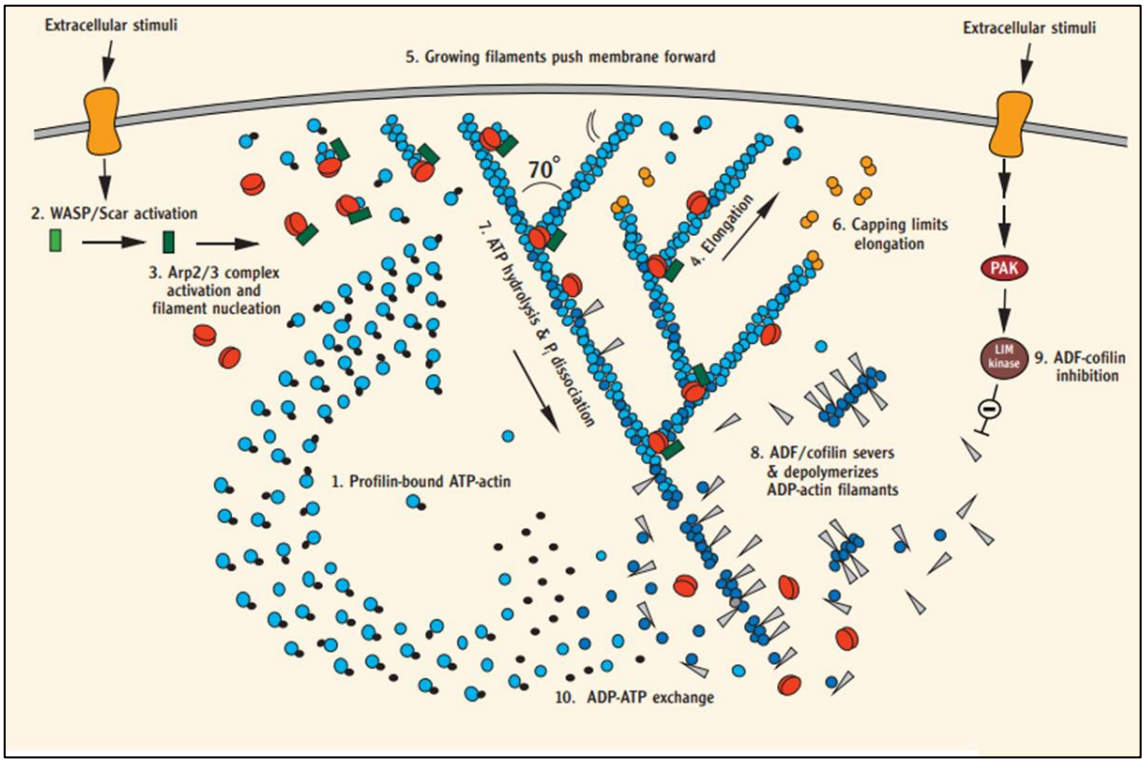


Figure 7 – Dendritic nucleation model for formation of F-actin networks. Adapted from (Pollard et al. 2001).

filaments to form, for example, lamellipodia. This network undergoes treadmilling as a whole, with filament nucleation and assembly occurring at the front (leading edge) and disassembling occurring at the back. The action of the actin depolymerizing factor cofilin is essential for disassembly, as it binds preferentially to F-actin-ADP (Maciver et al. 1994) and along the length of the filament, inducing mechanical stress that weakens and destabilizes it (De La Cruz 2009). Another important protein in cytoskeleton dynamics is profilin, a small protein that binds G-actin and accelerates the ADP-ATP exchange, replenishing the G-actin-ATP pool in the cell and thereby promoting its addition to the + end of growing F-actin (Goldschmidt-Clermont et al. 1992; Witke 2004). This process is to a large extent regulated by extracellular stimuli that activate proteins of the Rho GTPase family.

3.2 The small Rho GTPases family

GTPases are molecular switches that cycle between two conformational states, one active ("on") and GTP-bound, and the other inactive ("off") and GDP-bound. They only recognise targets when in the active state and are capable of GTP hydrolysis, rendering themselves inactive. The Ras superfamily is the most well studied and is composed by small and monomeric GTPases that can be divided into 5 main families, including the small Rho GTPases. In mammals, 22 different low molecular weight proteins (20-25 kDa) are part of this family (*Figure 8*) and regulate several cellular processes mostly related to actin cytoskeleton dynamics. They are simple in terms of structure, consisting mainly of a GTPase domain and a C-terminal CAAX box containing a cysteine residue that becomes prenylated allowing for membrane attachment (Ridley 2006). The small Rho GTPase family also comprises atypical members that are always found in the GTP-bound state and are regulated by different mechanisms (Etienne-Manneville et al. 2002; Heasman et al. 2008; Ridley 2006)

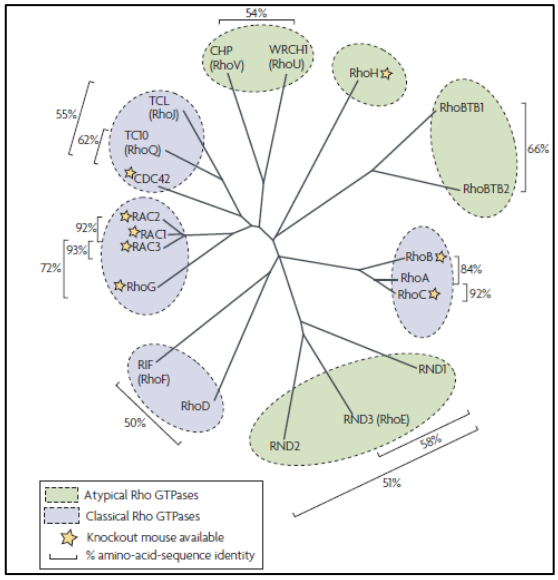


Figure 8 – Phylogenetic tree of the Ras superfamily of GTPases and respective subfamilies. Adapted from (Heasman et al. 2008)

The different mechanisms for regulation of classical Rho GTPases rely on guanine nucleotide exchange factors (GEFs), the GTPase activating proteins (GAPs) and the guanine nucleotide dissociation inhibitors (GDIs) (*Figure 9*).

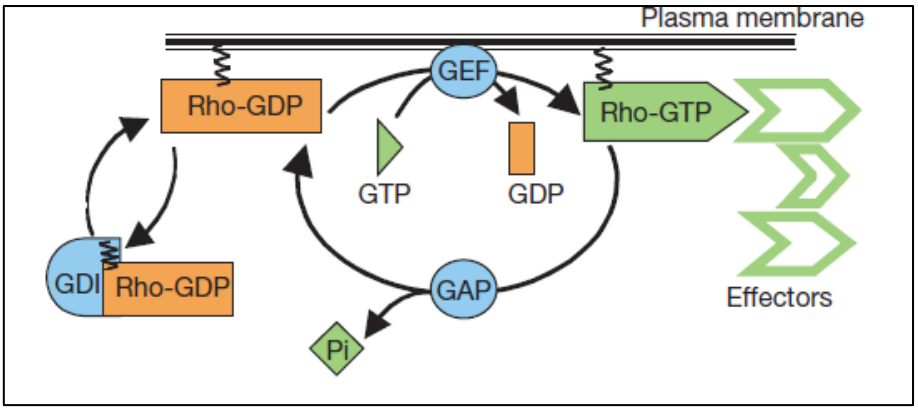


Figure 9 – Different mechanisms for regulation of Rho GTPase activity. Adapted from (Etienne-Manneville et al. 2002).

GEFs catalyse the exchange of GDP for GTP, mediating activation (Schmidt et al. 2002), while inactivation results from the action of GAPs that stimulate GTP hydrolysis (Moon et al. 2003), and GDIs, which inhibit attachment to the plasma membrane by interacting with the prenylated GDP-bound forms (Olofsson 1999). To a less extent, the biological activity of Rho GTPases can also be regulated by C-terminal modifications that influence their intracellular localization, phosphorylation, ubiquitination, protease cleavage and internalization (Bustelo et al. 2007).

It is well established that RhoGTPases control actin cytoskeleton dynamics. RhoA, Rac1 and Cdc42 are the most well studied proteins in this context. Early *in vitro* experiments in fibroblasts showed that overexpression of Rac1 induces formation of lamellipodia, while overexpression of Cdc42 leads to filopodia formation. On the other hand, overexpression of RhoA favours the formation of contractile stress fibres (Hall 1998). These three proteins can cooperatively control actin dynamics via many distinct signalling pathways. For example, regulation of cofilin by phosphorylation of LIM kinases (LIMKs); RhoA activates ROCK (Rho-associated protein kinase) (Ohashi et al. 2000) while Rac1/Cdc42 activate the serine-threonine kinases PAK (p21-activated kinase) (Edwards et al. 1999) which in turn activate LIMKs that phosphorylate and inactivate cofilin, leading to lamellipodia extension. Cross-talk between RhoA, Rac1 and Cdc42 is quite extensive and is mediated by either GEFs/GAPs/GDIs or downstream signalling pathways (Guilluy et al. 2011). Through these interactions, RhoA, Rac1 and Cdc42 can act synergistically or antagonize each other, creating a complex molecular dialogue that is highly regulated in space and time (*Figure 10*). The role of Rho GTPases in radial sorting and peripheral nerve development is further discussed ahead. Other common effectors of these proteins are the neural Wiskott-Aldrich syndrome (N-WASP) and WASP family Verprolin-homologous (WAVE) family of proteins. Both Cdc42 and Rac1 activate them leading to activation of the Arp2/3 complex (Takenawa et al. 2007).

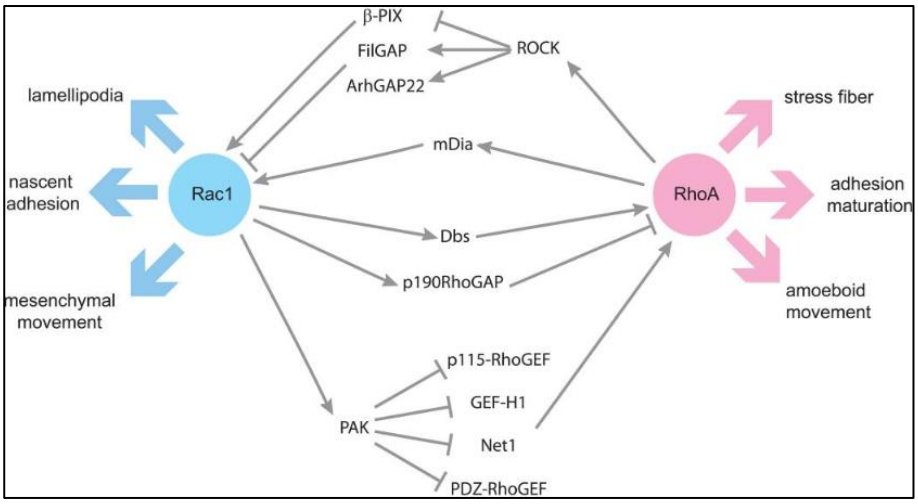


Figure 10 – Cross-talk between Rac1 and RhoA. Adapted from (Guilluy et al. 2011).

3.2.1. The RhoA subfamily

The RhoA subfamily includes the three highly homologous RhoA, RhoB and RhoC. Although they were characterized at the same time, RhoA is more widely studied. In humans, all three subtypes are expressed in all tissues with varying abundances depending on tissue type. Their primary protein sequences are around 85% identical, the C-terminus being the most diverse region (Wheeler et al. 2004). Since this region is critical in determining their intracellular localization it is expected that they are targeted to different regions of the cell. In fact, RhoB can be prenylated either with a farnesyl or a geranylgeranyl and localizes mainly on endosomes and lysosomes. RhoA and RhoC can only be geranylgeranylated and are usually found bound to the plasma membrane or in the cytosol (Adamson et al. 1992). Additionally, a small degree of sequence divergence is observed in regions that interact with regulators and target proteins, resulting in different affinities (*Table 3*) (Wheeler et al. 2004). This suggests that although members of the RhoA subfamily have high sequence homology, there are differences in terms of intracellular localization and interaction with effectors that may contribute for subtype-specific functions. Nevertheless, some degree of redundancy is to be expected.

Table 3 – Interaction between each Rho subtype and some effectors (by yeast 2 hybrid or pull down). + = mild interaction; ++ = moderate interaction; +++ = strong interaction; ? = unknown Adapted from (Wheeler et al. 2004).

Rho effectors			
Effector	RhoA	RhoB	RhoC
Rock 1+2	++	+	+++
mDia	++	+	++
PRK1/2 PKN	++	++	++
Rhoteckin	+++	+	+++
Rhophillin	+++	+	++
Kinectin	+++	?	?
Citron Kinase	++	+	+++
MBS	+++	?	?
p76RBE	+	++	?
PKC epsilon	++	++	+++
DBl transcription factor	+	++	?

3.3. Rho GTPase signalling in developmental myelination

During radial sorting SCs extend processes into axon bundles in order to segregate the larger ones to the periphery (Feltri et al. 2016; Webster et al. 1973). This requires the formation of lamellipodia radially in relation to the SC main axis that are able to contact with axons in immature bundles and segregate them (Nodari et al. 2007). Small Rho GTPases play a major role during developmental myelination in the PNS, as SCs must undergo profound cytoskeletal rearrangements. The expression of Rac, Cdc42 and RhoA in the sciatic nerve is characterized (Terashima et al. 2001) and their active levels seem to be developmentally regulated during the early postnatal period (*Figure 11*): levels of active Rac1 increase at P5, while RhoA levels greatly decrease and Cdc42 levels remain relatively unchanged. In adult nerves, active RhoA levels increase, while active Rac1 and Cdc42 levels remain stable (Nodari et al. 2007).

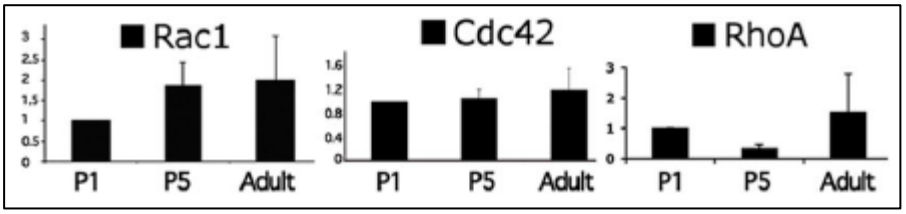


Figure 11 – Relative levels of active Rac1, Cdc42 and RhoA in sciatic nerves from wild-type mice. P5 and adult levels were normalized to P1 levels. Adapted from (Nodari et al. 2007).

In vivo experiments using conditional knockout mice showed that Rho GTPase signalling is critical in the response to ECM signals during SC development and myelination. Early embryonic ablation of *Rac1* specifically in SCs impairs process extension and stabilization required for lamellipodia formation, culminating in radial sorting defects and hypomyelination (Benninger et al. 2007). Mechanistically, in these mutants the ECM-β1 integrin intracellular signalling response is disrupted (Nodari et al. 2007). Additionally, deletion of integrin-linked kinase (ILK), an obligatory component of the IPP (ILK-PINCH-Parvin) complex that mediates integrin signalling, leads to a very similar phenotype. This study also concluded that ILK-mediated inhibition of Rho/ROCK signalling is required for radial sorting to occur (Pereira et al. 2009). Cdc42 is also required for radial sorting and myelination because it regulates SC proliferation in response to NRG1 signalling (Benninger et al. 2007).

Other actin-related proteins have also been shown to differentially regulate developmental myelination of the PNS. Conditional deletion of Profilin 1, which gets phosphorylated and thus inactivated by ROCK (Shao et al. 2008), leads to radial sorting and myelination defects due to deficient lamellipodia formation (Montani et al. 2014). In contrast, mice lacking N-WASP are capable of sorting axons but are arrested at the pro myelinating stage and do not begin to myelinate (Novak et al. 2011), suggesting that it

is essential for SC membrane wrapping. Another substrate of ROCK (Amano et al. 1996) implicated in actin cytoskeleton remodelling in SCs is myosin II. Upon activation by phosphorylation, myosin light chain (MLC) induces the formation of contractile actomyosin fibres. It has been suggested that this activation is downregulated at the beginning of myelination, as a reduction of contractile stress fibres leads to an increase in cell membrane extension and spreading, a process linked to proper axon ensheathment (Leitman et al. 2011).

Cofilin1, an actin filament disassembly and severing factor (figure 12), has also been shown to have a role in myelination. *In vitro* experiments suggest that the activity of cofilin1 is tightly regulated in a spatio-temporal way to allow stabilization of F-actin (cofilin inactivation) during engagement of axons by SCs, followed by directed expansion of cell membrane during active myelination (cofilin activation) A model for cofilin function during SC myelination proposes that cofilin is inactivated by phosphorylation during axon engagement and SC alignment, mediated by β1 integrin/Rho GTPase signalling. Subsequently, basal lamina deposition clusters β1 integrin along the abaxonal (further from the axon) plasma membrane, while axonal NRG1 activates ErbB2/B3 receptors in SCs along the adaxonal (closer to the axon) plasma membrane, resulting in cofilin dephosphorylation (Sparrow et al. 2012). This polarization in cofilin activity allows for the expansion of the SC adaxonal plasma membrane required during active myelination, while the abaxonal portion is stabilized by cofilin inactivation.

3.3.1. RhoA in SC biology and sciatic nerve development

A role for Rho/ROCK signalling during the early stages of myelination has been previously explored (Melendez-Vasquez et al. 2004). This study, using an *in vitro* approach, showed that ROCK inhibits process extension in SCs and regulates branching and myelin sheath organization, particularly the node of Ranvier. Another study also showed that inhibition of ROCK in ILK-null SCs restored process extension and rescued the radial sorting defects observed in ILK mutants (Pereira et al. 2009). These two studies suggest that Rho/ROCK activity is downregulated at the onset of radial sorting. In contrast, GPR56, a G protein-coupled receptor from the adhesion class expressed in SCs, was recently shown to be a regulator of radial sorting through RhoA activation and actin cytoskeleton remodelling (Ackerman et al. 2018). The authors hypothesized that this activation is important for formation of actin stress fibres and SC adhesion to axonal membranes during axon engagement. This indicates that RhoA activation must be tightly regulated during PNS development.

Two other recent studies, where lentivirus-mediated RNA interference was used to locally downregulate the expression of RhoA in rat sciatic nerve and in SCs *in vitro*,

showed that: 1) RhoA is required for proliferation and migration of SCs *in vitro*; 2) regulates SC differentiation, as both *in vitro* studies and analysis of injected sciatic nerves showed that RhoA inhibition impairs differentiation through activation of JNK (c-Jun N-terminal kinase; and 3) injected sciatic nerves displayed a hypomyelination phenotype (Wen et al. 2017; Wen et al. 2018).

These studies point to an important role of RhoA in PNS development (*Figure 12*). However, the function of RhoA in myelination has not been assessed *in vivo* and given the complexity of the Rho-associated signalling pathways, what specific cellular processes (proliferation, differentiation and cell shape) are specifically regulated by RhoA in SCs remains poorly understood.

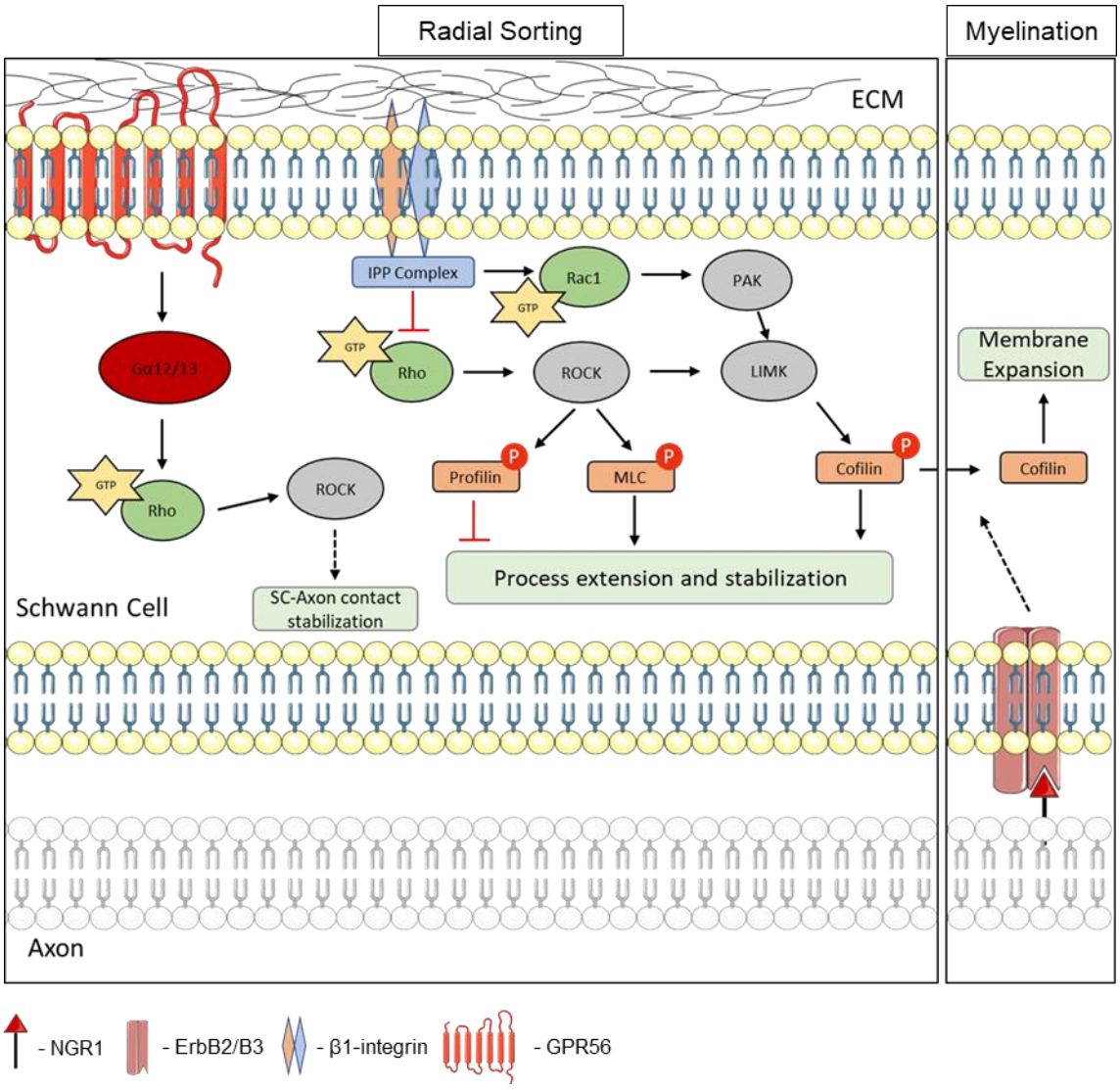


Figure 12 – Simplified overview of molecular pathways involving Rho signalling and related to the actin cytoskeleton, radial sorting and myelination.

4. Previous findings

Before the start of this Masters thesis project, PNS myelination was analysed by electron microscopy (EM). Morphometric analysis was used to quantify a set of parameters that assess radial sorting and onset of myelination. This includes the number of total single sorted fibres, of SCs in a 1 to 1 relationship with axons (from now on referred to as "1-to-1s") and of myelinated axons. This quantitative analysis gave us a picture of the early postnatal stages of peripheral nerve development: segregation of axons to the periphery of immature bundles, acquisition of a 1-to-1 relationship between SCs and axons and myelination, respectively (*Figure 2*).

4.1. Analysis of the early postnatal stage

Sciatic nerve crossections obtained from P1 (*Figure 13A*) and P5 (*Figure 13E*) mice where RhoA was conditionally ablated in myelinating cells (detailed information about the animal model used in this work is available in Chapter II: materials and methods) were used to analyse the early postnatal stages of peripheral nerve development.

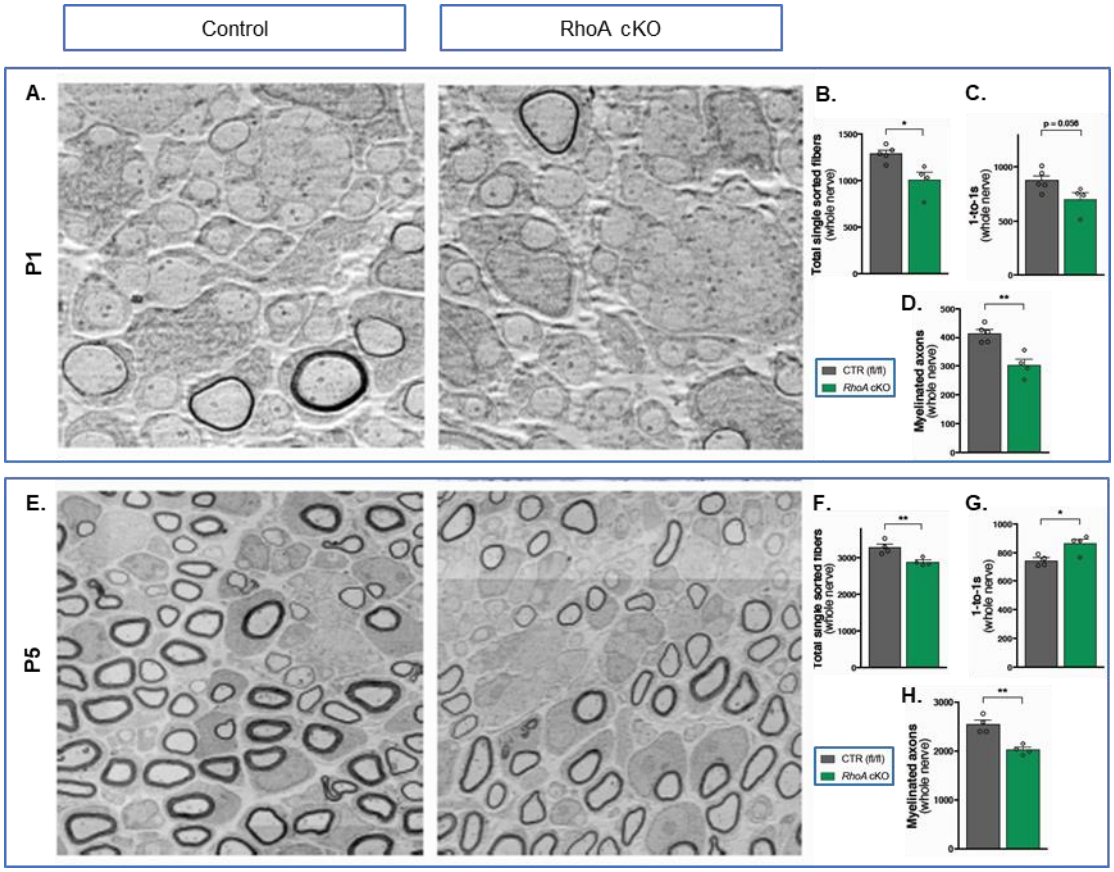


Figure 13 – EM images of crossections obtained from P1 (A) and P5 (E) littermates and subsequent morphometric analysis shows a radial sorting delay in RhoA cKO. A set of parameters related to radial soring and onset of myelination were determined for both timepoints. These are the number of total single sorted fibres (B and F), of 1-to-1s (C and G) and of myelinated axons (D and H). Error bars indicate ± SEM. *, P <0,05; **, P<0,01.

In P1 sciatic nerves from *RhoA* ckO the total number of sorted (*Figure 13B*) and myelinated axons (*Figure 13D*) was decreased when compared to control littermates. The number of 1-to-1s showed a tendency to be decreased in *RhoA* ckO (p=0.056; *Figure 13C*). At P5, the total number of sorted axons (*Figure 13F*) is still decreased in RhoA mutants, possibly indicating a radial sorting defect. At this stage the number of myelinated axons (*Figure 13H*) was also decreased in RhoA mutants, while the number of 1-to-1s (*Figure 13G*) was increased when compared to control littermates. These observations suggest that the onset of myelination is delayed when RhoA is ablated in myelinating cells.

Quantitative PCR analysis of SC differentiation markers *Mbp* (*Figure 14A*), *Krox20* (*Figure 14B*) and *Oct6* (*Figure 14C*) in P1 sciatic nerves of *RhoA* ckO mice provided preliminary indication that RhoA appears to be dispensable for SC differentiation.

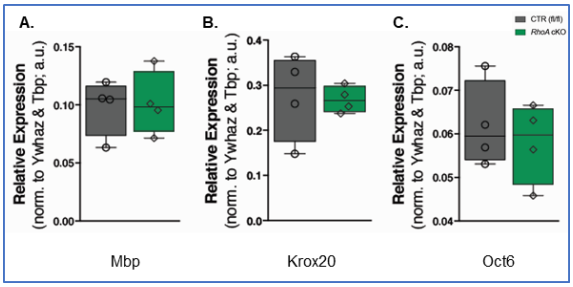


Figure 14 – Expression analysis of three SC differentiation markers, Mbp (A), Krox20 (B) and Oct6 (C) by quantitative real-time PCR in P1 sciatic nerves. Error bars indicate ± SEM.

4.2. Analysis of later stages of myelination

Morphometric analysis of P15 (*Figure 15A*) and P25 (*Figure 15C*) sciatic nerve crossections obtained from another mouse line (where a different promoter regulatory sequence (*Dhh-Cre)* was used to conditionally ablate RhoA specifically in SCs) showed

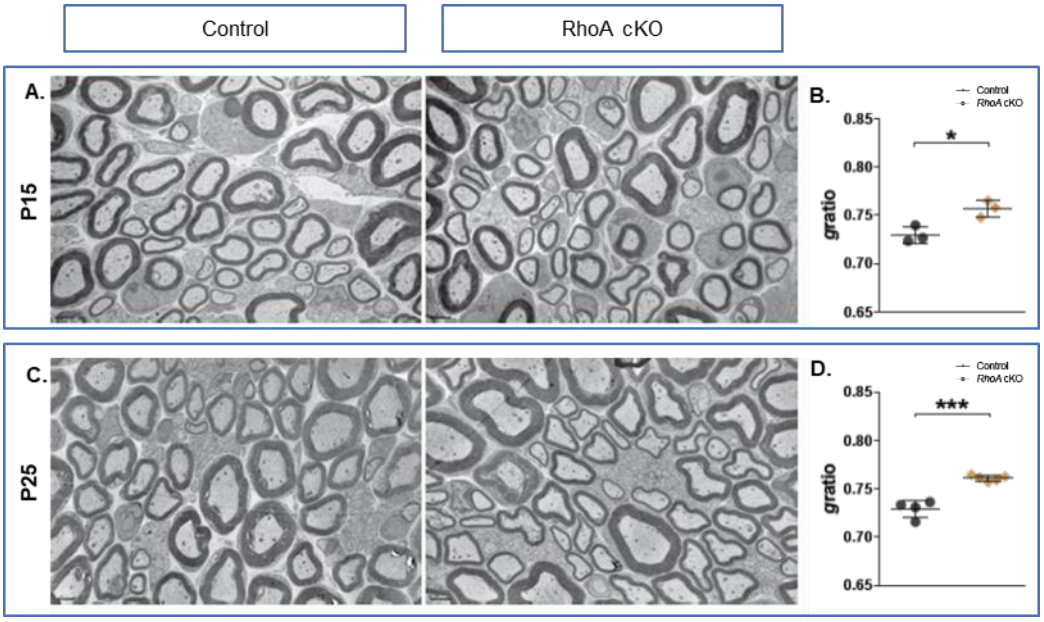


Figure 15 – EM images of crossections obtained from P15 (A) and P25 (C) littermates and subsequent morphometric analysis (B and D) shows a g-ratio increase in RhoA cKO sciatic nerves Error bars indicate ± SEM. *, P <0,05; ***, P <0,001.

that myelin thickness is decreased in the absence of RhoA, which is indicative of hypomyelination. However, further studies are required to assess if the phenotype results from a delay in the onset of myelination and/or radial sorting defects, or abnormal/decreased myelin production.

5. Aims

Previously published studies and the information available in the literature suggests that regulation of actin cytoskeleton dynamics is important for the control of the different steps in developmental myelination of the PNS. In particular, the ECM-integrin-Rho GTPase signalling pathway has been implicated in radial sorting regulation. But how?

To study the role of the small Rho GTPase RhoA in SC biology and myelination during peripheral nerve development *in vivo*, we used a conditional knockout mouse model where RhoA is ablated specifically in myelinating glia. To assess the functions of RhoA in Schwann cell biology we:

1) Analysed survival by TUNEL;
2) Used primary Schwann cell cultures and immunofluorescence to evaluate lamellipodia formation and process extension;
3) Performed western blot analysis to study signalling pathways related to actin cytoskeleton dynamics

To understand how RhoA regulates myelination *in vivo* we:

1) Performed Western blot analysis to assess the levels of MBP and investigate AKT signalling
2) Used immunofluorescence techniques to measure the internode length, a parameter associated with myelination

Chapter II: Materials and Methods

1. A conditional knockout mouse model for *RhoA*

In this study we used the Cre/lox recombinase system to generate a conditional knockout mouse model in which the *RhoA* gene is ablated specifically in myelinating cells (*Figure 16*). This system makes use of the P1 bacteriophage Cre (causes recombination) enzyme that catalyses specific recombination between the loxP-sites (locus of crossing over) that are inserted into specific locations in the gene of interest. In this case, homozygous mice carrying loxP elements flanking the third exon of the *RhoA* gene (*RhoA*$^{lox/lox}$) were crossed with mice carrying the *Cre* gene under the control of *2',3'-cyclic nucleotide 3'-phosphodiesterase* gene (*Cnp*) promoter, generated as previously described (Lappe-Siefke et al. 2003). Mice generated by this crossing will either be CNP-Cre^{+} *RhoA*$^{lox/lox}$ (express Cre recombinase - *RhoA* ablated - mutants) or CNP-Cre^{-} *RhoA*$^{lox/lox}$ (*RhoA* is intact – controls).

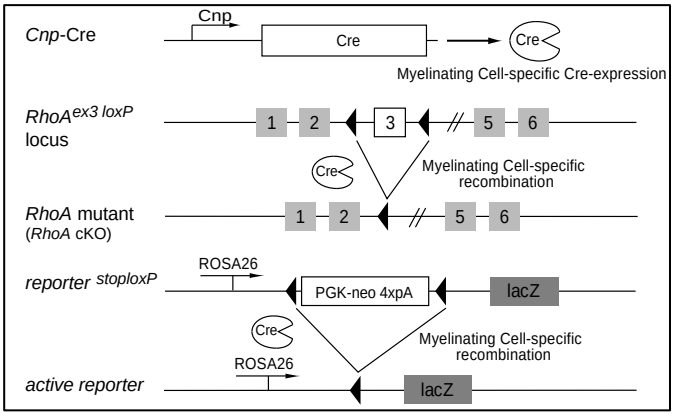


Figure 16 – Myelinating cell-specific ablation of RhoA using the Cre-Lox system.

Genotyping was performed following a previously published protocol (Jackson et al. 2011) by the Cell Culture and Genotyping (CCGen) service at i3S.

2. Tissue dissection

For this work the sciatic nerve was the tissue of choice, since it is the largest peripheral nerve and SCs are the major cell population.

To collect tissue for Western blot analysis, animals at different developmental stages (P5, P15 and P25) were euthanised before dissection. P15 and P25 animals were euthanized by asphyxia (in a CO_2 chamber) followed by decapitation, while P5 animals, since they are resistant to hypoxia, were decapitated.

To collect preserved tissue for immunofluorescence (IF) analysis, we performed whole animal transcardial perfusion fixation. Animals were anesthetized with an intraperitoneal injection of diluted sodium pentobarbital (recommended dose: 0.2mL per 30g of body weight) and once the animal reached a surgical plane of anaesthesia (evaluated by the tail pinch and pedal withdrawal reflexes), chest skin was removed, and the pleural cavity exposed. Afterwards, a venipuncture butterfly needle connected to the

perfusion pump was inserted into the posterior end of the left ventricle and passed to the ascending aorta and an incision was made in the right atrium. The animal was infused with PBS (phosphate-buffered saline) (~10-15mL for an adult), followed by the fixative solution (~30-35mL for an adult). The fixative used was a 4% paraformaldehyde (PFA-Sigma Aldrich) solution in PBS.

All guidelines regarding animal housing, breeding and welfare followed Portuguese Veterinary Office (DGAV) and European Union directives.

3. Preparation of total protein lysates from fresh tissue

Sciatic nerves were dissected out and stripped of perineurium and epineurium. Both nerves of each animal were pooled together and homogenized on ice with a chilled pestle in lysis buffer consisting of radioimmunoprecipitation assay buffer (RIPA; Sigma- 150mM NaCl; 0.5% sodium deoxycholate; 0.1% SDS; 50 mM Tris; IGEPAL CA-630; pH 8.0), 0.001M ethylenediaminetetraacetic acid (EDTA -Merck), 1% protease inhibitor cocktail (Sigma) and 1% phosphatase inhibitor cocktail (Sigma). Samples were then centrifuged at 1300 xg, 4ºC to clear the lysate, recovered and stored at - 80ºC.

4. Western blot analysis

Protein lysates were thermally denatured (10 min at 65ºC + 5 min at 95ºC) in a reducing mix of gel loading buffer (150mM Trizma Base-Fisher Scientific; 6% SDS-Sigma; 0.05% Bromophenol Blue- Alfa Aesar; 30% glycerol; 6nM EDTA- Merck; pH 8.8) and 1% DTT (Dithiothreitol-Promega). Protein concentration was not determined prior to loading, since the amount recovered from lysates was relatively low. Instead, we used 12 µL of protein lysate per well and a loading control to normalize the data. Proteins were separated by non-gradient denaturing SDS-PAGE (sodium dodecyl sulfate-polyacrylamide gel electrophoresis) with different percentages (8, 10 and 12%) depending on the molecular weight of the target protein to be analysed and using a stable electric current of 12 mA. Proteins were transferred into a nitrocellulose membrane using a semi-dry transfer system and transfer buffer/methanol mix (Trans-Blot Turbo system, Biorad) using a stable electric current of 1.2 mA for 12 minutes. Membranes were washed in Tris buffered saline (TBS pH=7.6; 0.2M Trizma Base; 8% sodium chloride-VWR), stained for total protein content with Ponceau S (Sigma) and afterwards blocked in 5% milk-TBS or 5% bovine serum albumin-TBS (BSA-Nzytech) for 1h at room temperature. Incubation with primary antibodies (*Table 4*) was performed overnight at 4ºC in blocking solution and with rotation with roughly 125 µL antibody solution/cm^2 of membrane. To remove unbound primary antibody, membranes were washed 3x for 10 minutes with TBS-T (TBS with 0.1% Tween 20-Fisher Scientific). Incubation with

secondary antibodies (*Table 5*) was performed at room temperature for 1h in blocking solution, followed by 3x 10-minute washes. These antibodies are conjugated with horseradish peroxidase (HRP) allowing for chemiluminescent detection using a ChemiDoc XRS+ (Biorad) system. Immunoblots were developed by incubating membranes with SuperSignal West Pico Plus Chemiluminescent Substrate solution (Thermo Fisher) for 5 minutes. Images were obtained using ImageLab software (Biorad).

Some membranes were stripped of antibodies for re-probing. This was done by washing the membranes with mild stripping solution (200 mM glycine -Fisher BioReagents; 3.5 mM SDS; 1% Tween 20; pH=2.2) 2x for 10 minutes, followed by 2x 10-minute washes with phosphate buffered saline (PBS: 8% sodium chloride; 2.68% di-sodium hydrogen phosphate - Merck; 0.2% sodium chloride; 0.24% potassium hydrogen phosphate - Alfa Aesar) and 2x 5-minute washes with TBS-T. After incubation with blocking buffer for 1h at room temperature, membranes were incubated with primary antibodies as described above.

4.1. Quantification of WB signal

Western blot image acquisition was performed using Image Lab 5.2.1 software (Biorad). For quantification of signal intensity, Image J Fiji Software (Schindelin et al. 2012) was used. Only images where the signal was not saturated were used for quantification.

5. Tissue preparation for immunofluorescence analysis

5.1. Frozen sections

Sciatic nerves were dissected out as described above and post-fixed overnight in a 4% PFA solution at 4ºC. Afterwards, nerves were changed into a solution of 20% sucrose overnight, embedded in optimal cutting temperature medium (OCT; Cryomatrix – Thermo Fisher), sectioned longitudinally into 12 µm sections using a cryostat (Cryostat Leica CM 3050S), mounted onto SuperFrost Plus (Thermo Scientific) microscope slides, dried at room temperature and stored at -80ºC until use.

5.2. Teased fibres

Sciatic nerves from P25 mice were fixed *in situ* by injecting a 4% PFA solution in PBS directly into the sciatic nerve pocket, dissected out and fixed overnight in 4% PFA in PBS at 4ºC. The epineurium and perineurium were removed using fine forceps and a 0.5-1 mm nerve segment was cut using spring scissors, in PBS and under a stereomicroscope. The nerve segment was transferred into a microscope slide coated with 3-aminopropyltriethoxysilane (APES -Sigma), teased using fine needles until individual

fibres were isolated, dried at room temperature and stored overnight at 4ºC for stronger adhesion.

6. Primary cultures of Schwann cells

Sciatic nerves from P4 mice were collected under sterile hood and stripped from perineurium and epineurium in Hanks' balanced salt solution (HBSS-SIGMA). Tissue was digested with collagenase (4 mg/ml -Sigma) and hyaluronidase (1.2 mg/ml) prepared in minimum essential medium (MEM -Sigma) and in the presence of trypsin inhibitor (10 mg/ml -Sigma). Enzymatic digestion was performed at 37ºC for 70 minutes and then stopped with Dulbecco's modified Eagle's medium (DMEM -Gibco) with 10% fetal calf serum (FCS -Gibco). The solution was resuspended by pipetting it up and down until no nerve aggregate was visible, centrifuged at 1200 rpm for 5 minutes and the digestion media (supernatant) discarded. The cells were resuspended in DMEM with 2% B27 and 0.5% FCS and seeded in glass coverslips coated with 25 µg/mL Poly-D-lysine (PDL -Sigma) and 0.2 µg/mL merosin/Laminin (Grupo Taper-PG+HITEC). Cells were maintained at 37ºC with 5% CO_2 in a tissue culture incubator for 24h.

7. Immunofluorescence analysis

7.1. Immunohistochemistry of teased fibres

For immunostaining of teased fibres, sections were washed two times for 5 minutes in PBS, permeabilized for 30 minutes with 2.5% Triton X-100 (VWR) in PBS and blocked for 1h at room temperature with a 1% normal goat serum (Invitrogen), 1% horse serum (Gibco) and 1% HEPES (Merck) buffer solution in PBS. Incubation with primary antibody that recognises contactin-associated protein (Caspr) (*Table 4*) was done in blocking solution, overnight, at 4ºC and in a dark humidified chamber. After incubation, fibres were washed 3x for 5 minutes with a 0.025% Triton X-100 solution in PBS and incubated with secondary antibodies (*Table 5*) in blocking solution, for 1h at room temperature and in a dark humidified chamber, followed by a 10-minute incubation with 4′,6-diamidino-2-phenylindole (DAPI - Alfagene). Fibres were then washed with PBS and mounted with Fluoroshield (Sigma Aldrich). Image acquisition was done the following day.

7.2. TUNEL staining

The TUNEL assay (terminal deoxynucleotidyl transferase dUTP nick end labelling) relies on the action of the enzyme TdT (terminal deoxynucleotidyl transferase) that catalyses the addition of dUTPs labelled with biotin to the free 3' ends that result from double-strand breaks in the DNA formed during apoptosis (Gavrieli et al. 1992). Biotin is

subsequently stained with streptavidin coupled to a fluorophore. This allows for the detection of apoptotic nuclei in crossections of fixed tissue.

Sciatic nerve longitudinal frozen sections were blocked for 1h with 10% normal goat serum, 0.1% BSA and 1% Triton X-100 in PBS, washed 3 times for 5 minutes with PBS and equilibrated in terminal deoxynucleotidyl transferase buffer (TdT - pH=7.2; 30 mM Tris-HCl, 140 mM sodium cacodylate trihydrate -Sigma; 1mM cobalt (II) chloride hexahydrate -Alfa Aesar) for 10 minutes at room temperature. The enzymatic reaction for integration of biotin-labelled UTP was done for 1.5h at 37ºC in a moist chamber with a reaction mix consisting of biotin-16-dUTP (Roche), TdT enzyme (Roche) and dATP (Promega). The reaction was stopped by adding 2x SSC buffer (saline-sodium citrate) for 10 minutes, followed by 3x 5 minutes wash in PBS and incubation with streptavidin conjugated with AlexaFluor 568 (*Table 5*) in a 10% normal goat serum, 0.05% Triton X-100 solution in PBS for 1h at room temperature in a dark, moist chamber. Lastly, sections were washed 3 times in PBS for 5 minutes, incubated for 15 min with DAPI, washed again and mounted with Fluoroshield. Image acquisition was performed the following day.

7.3. Immunocytochemistry

Primary SCs were quickly washed with PBS, fixed with 4% PFA in MP (microtubule protecting) buffer (65 mM PIPES -Millipore; 25 mM HEPES -Sigma; 10mM EGTA -Sigma; 3 mM $MgCl_2$ -Sigma;) for 10 minutes at room temperature, washed again in PBS and permeabilized with 0.2% Triton-X100 in PBS for 10 minutes. Blocking was done with a 10% goat serum in PBS solution, for 1h at room temperature, followed by incubation with primary antibodies specific to RhoA and tubulin (*Table 4*) overnight at 4ºC in blocking buffer. Cells were then washed with PBS and incubated with secondary antibodies and phalloidin (*Table 5*) for 1h at room temperature and in a dark chamber. After washing with PBS, cells were incubated with DAPI for 10 min, washed again, mounted with Fluoroshield and stored at 4ºC overnight. Image acquisition was performed the following day.

8. Image acquisition and processing

For immunofluorescence image acquisition, a motorized inverted DMI 6000B epifluorescence microscope (Leica, Wetzlar, Germany) equipped with a digital ORCA-Flash4.0 vs2 Digital CMOS camera (C11440-22CU, Hamamatsu Photonics, Japan) was used. Images were processed using Image J Fiji software (Schindelin et al. 2012). Internode and SC process length were measured using Image J measure tool. The cell

counter plugin of Image J was used for lamellipodia and TUNEL-positive nuclei quantification. All quantifications and measurements were performed blindly.

9. Statistical analysis

Statistical analysis was performed using GraphPad 6.0 Prism software. Data distribution was tested for normality using the Shapiro-Wilk test. Statistical significance between groups of measurements that follow a normal distribution and pass the F test of variances was determined using a two-tailed Student's *t* test. For process length distribution results, multiple t tests, one for each interval, were performed.

Table 4 – List of primary antibodies used for Western blot and Immunofluorescence

Antibody	Company/Catalog number	Dilution	Host
Akt	Cell Signaling Technology; #9272	1:1000	Rabbit polyclonal
p-Akt Thr 308	Cell Signaling Technology; #2965	1:1000	Rabbit monoclonal
p-Akt Ser 473	Cell Signaling Technology; #4051	1: 1000	Mouse monoclonal
Cofilin	Abcam; #ab54532	1: 2000	Mouse monoclonal
p-Cofilin Ser 3	Abcam; #ab12866	1: 1000	Rabbit polyclonal
GAPDH	HyTest; #6C5	1:50 000	Mouse monoclonal
MBP	Abcam; #ab7349	1:500	Rat monoclonal
Profilin-1	Abcam; #ab50667	1: 1000	Rabbit polyclonal
p-Profilin	(Shao et al. 2008); kindly provided by the Nerve Regeration group at I3S	1: 1000	Rabbit polyclonal
RhoE/Rnd3	Millipore; #05-723	1: 500	Mouse monoclonal
ROCK1	Abcam; #ab134181	1: 500	Rabbit monoclonal
ROCK2	Abcam; #ab125025	1: 2000	Rabbit monoclonal
α-Tubulin	Sigma; #T5168	1: 10 000	Mouse monoclonal
CASPR	NeuroMab; #75-001	1: 200	Mouse monoclonal
RhoA	Santa Cruz; #SC-418	1:200	Mouse monoclonal

Table 5 – List of secondary antibodies and molecular probes used for Western blot and Immunofluorescence

Antibody	Company/Catalog number	Dilution	Host
Peroxidase-Conjugated AffiniPure Donkey Anti-Rabbit IgG	Jackson ImmunoResearch; #711-035-152	1:10 000	Donkey polyclonal
Peroxidase-Conjugated AffiniPure Goat Anti-Mouse IgG	Jackson ImmunoResearch; #115-035-146	1:15 000	Goat polyclonal
Peroxidase-Conjugated AffiniPure Goat Anti-Rat IgG	Jackson ImmunoResearch; #112-035-003	1:10 000	Goat polyclonal
AlexaFluor 488 anti-mouse	Invitrogen; #A21202	1: 1000	Donkey polyclonal
AlexaFluor 594 Phalloidin	Invitrogen;#A12381	1:50	-
AlexaFluor 568 Streptavidin	Alfagene; #S11226	1: 1000	-

Chapter III: Results and discussion

1. A Schwann cell-specific knockout mouse model for *RhoA*

Ablation of RhoA specifically in SCs was confirmed by Western blot and immunofluorescence analysis of primary SCs isolated from sciatic nerves of neonate mice (*Figure 17)*. Expression levels of total RhoA were significantly lower in sciatic nerve lysates obtained from RhoA cKO P5 mice when compared to control littermates (*Figure 17B*). Immunocytochemistry (ICC) analysis was performed to detect RhoA in primary SCs obtained from control and RhoA mutant sciatic nerves. With this antibody, expression of RhoA was not detected in SCs isolated from RhoA mutants (*Figure 17A*).

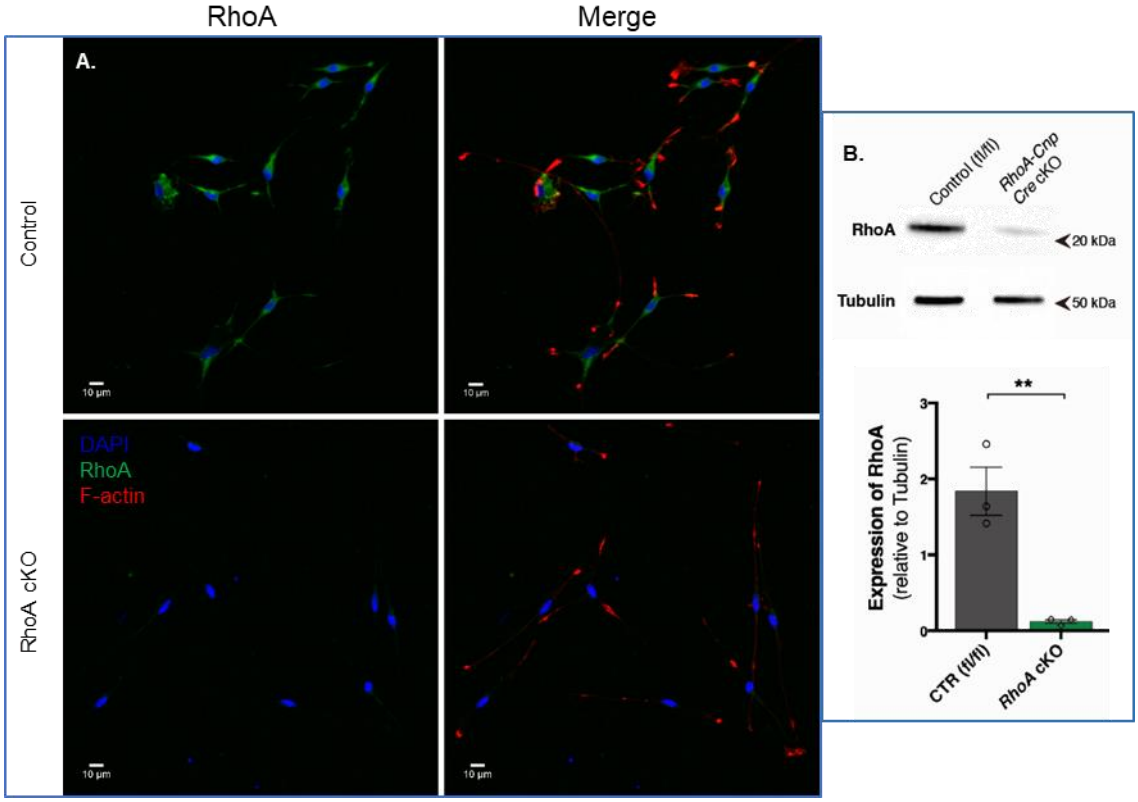


Figure 17 – RhoA was successfully ablated in RhoA-Cnp Cre cKO. (A) ICC of primary SCs obtained from RhoA cKO sciatic nerves and (B) Western blot analysis of P5 sciatic nerves obtained from control (n=3) and RhoA cKO (n=3) littermates showed that RhoA expression is significantly lower in mutant sciatic nerves. Error bars indicate ± SEM. **, p <0.01.

2. RhoA regulates radial sorting and the onset of myelination

Ultrastructural analyses performed previously to the start of this Masters thesis (described in chapter I: Introduction, pages 19-21) suggest that RhoA may play an important role during peripheral nerve development, especially during the early postnatal period. Radial sorting was found to be delayed in RhoA cKO (*Figure 13*), with an hypomyelination phenotype being present at later stages (*Figure 15*). These findings

could be attributed to impairment in various processes: differentiation of SCs, proliferation and/or survival (SCs fail to timely establish a 1-to-1 relationship with axons) or cytoskeletal defects (SCs fail to segregate axons from immature bundles). Quantitative PCR analysis was previously performed and showed that RhoA is probably dispensable for SC differentiation (*Figure 14*). Therefore, we aimed at understanding what process(es is impaired upon depletion of RhoA that could explain the developmental defects observed in RhoA ckO.

2.1. RhoA is dispensable for early post-natal survival of SCs

TUNEL assay was used to identify apoptotic SCs in P5 sciatic nerves. TUNEL-positive nuclei were counted and normalized to the total number of SC nuclei, determined by DAPI staining. The results show that the rate of apoptosis was low in controls (similar to what is described in the literature (Benninger et al. 2007)) and appears to be slightly decreased in mutants (*Figure 18*). This suggests that RhoA is dispensable for SC survival in early post-natal sciatic nerves. Therefore, next we decided to evaluate if radial sorting impairment could be attributed to cytoskeletal defects.

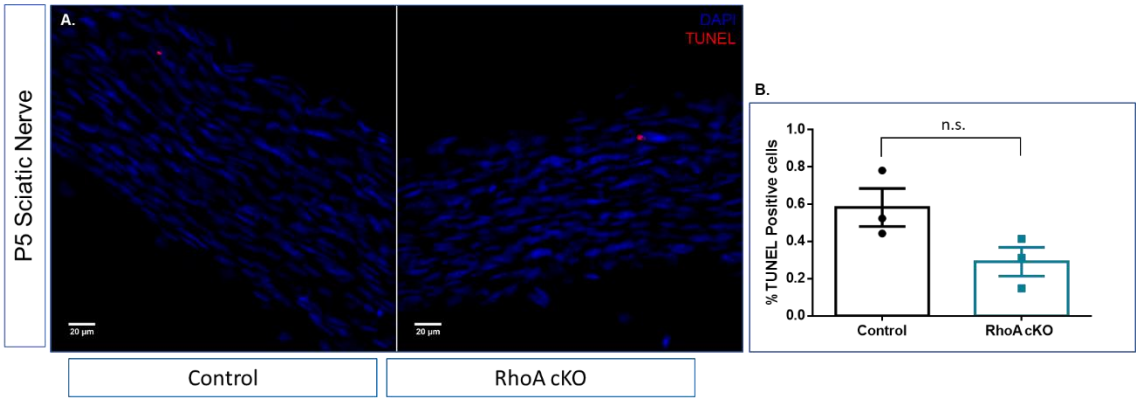


Figure 18 – RhoA appears to be dispensable for early post-natal survival of SCs. (A) Representative images of TUNEL staining of P5 sciatic nerves longitudinal sections and (B) quantification of TUNEL positive cells. The rate of apoptosis is low and does not appear to be altered between control (n=3) and mutant (n=3) littermates. Error bars indicate ± SEM.

2.2. Process extension is impaired in mutant SCs

As previously stated, the formation of lamellipodia radially in relation to the cell main axis by SCs is essential for axon segregation during radial sorting (Webster et al. 1973). This change in cell shape is regulated by extracellular matrix laminins, that signal through β1 integrin receptors in SCs. SC-specific ablation of β1 integrin leads to radial sorting impairment caused by defects in process extension and maintenance (Feltri et al. 2002). In β1 integrin-null SCs, elongation and migration along the axon occurs normally but extension of radial lamellipodia is impaired. This impairment is Rac1 dependent, as Rac1-GTP levels are significantly reduced and injection with an adenovirus expressing

constitutively active Rac1 improved axonal sorting in β1 integrin-null nerves (Nodari et al. 2007). In line with this, morphological studies using a conditional knockout mouse for Rac1 also showed that process extension and stabilization in SCs is defective and that the radial sorting defects observed are a consequence of this impairment (Benninger et al. 2007). ILK-cKO (with SC-specific ablation of ILK) is another conditional knockout mouse model where radial sorting and PNS myelination is severely impaired due to deficits in SC process extension (Pereira et al. 2009). *In vitro* studies showed that ILK-null SCs have significantly shorter processes compared to controls and that treatment with ROCK inhibitors increases the number of SCs with longer processes. In fact, Rho (RhoA, B and C) activity was found to be significantly increased in *ILK* cKO sciatic nerves and injection with a ROCK inhibitor re-established radial sorting, suggesting that increased Rho/ROCK signalling was associated with a decrease in process extension.

To evaluate if the formation of lamellipodia, as well as axial process extension was impaired in SCs from RhoA cKO, SCs obtained from P4 sciatic nerves were seeded for 24h and labelled with anti-tubulin antibody and phalloidin (*Figure 19A*). Phalloidin is a bicyclic peptide that belongs to a family of toxins isolated from *Amanita phalloides* (Wulf et al. 1979). It selectively binds F-actin and can be used, when conjugated with a fluorochrome, to visualize the actin cytoskeleton in fixed cells (Small et al. 1999).

Quantification of the number of axial (*Figure 19B*) and radial (*Figure 19C*) lamellipodia formed per SC showed that, in the absence of RhoA, SCs extend less radial lamellipodia, while the number of axial lamellipodia remains unchanged. This suggests that perhaps SCs are unable to correctly extend processes into immature axon bundles in the beginning of radial sorting. Axial lamellipodia are implicated in directional migration of cells, and so the fact that their number isn't altered in SCs derived from RhoA cKO could suggest that SC migrate normally along axons. Pull-down analysis of P5 sciatic nerve lysates showed that expression of Rac1 is upregulated in RhoA mutant nerves while the levels of active Rac1 levels decrease significantly in mutants (*Figure 19E*). This suggests that RhoA could be important for Rac1 activity in SCs.

The length of axial processes was also measured. Control and mutant SCs were categorized according to process length and their relative percentage in each category was calculated *(Figure 19D*). Results show that there is a higher frequency of SCs with longer processes in RhoA mutant SCs, confirming previous reports that Rho activity regulates process length in SCs (Pereira et al. 2009).

These findings suggest that there is an impairment in the transition of SCs between migration/elongation along axons and axon segregation/wrapping. This could contribute for the radial sorting delay previously observed.

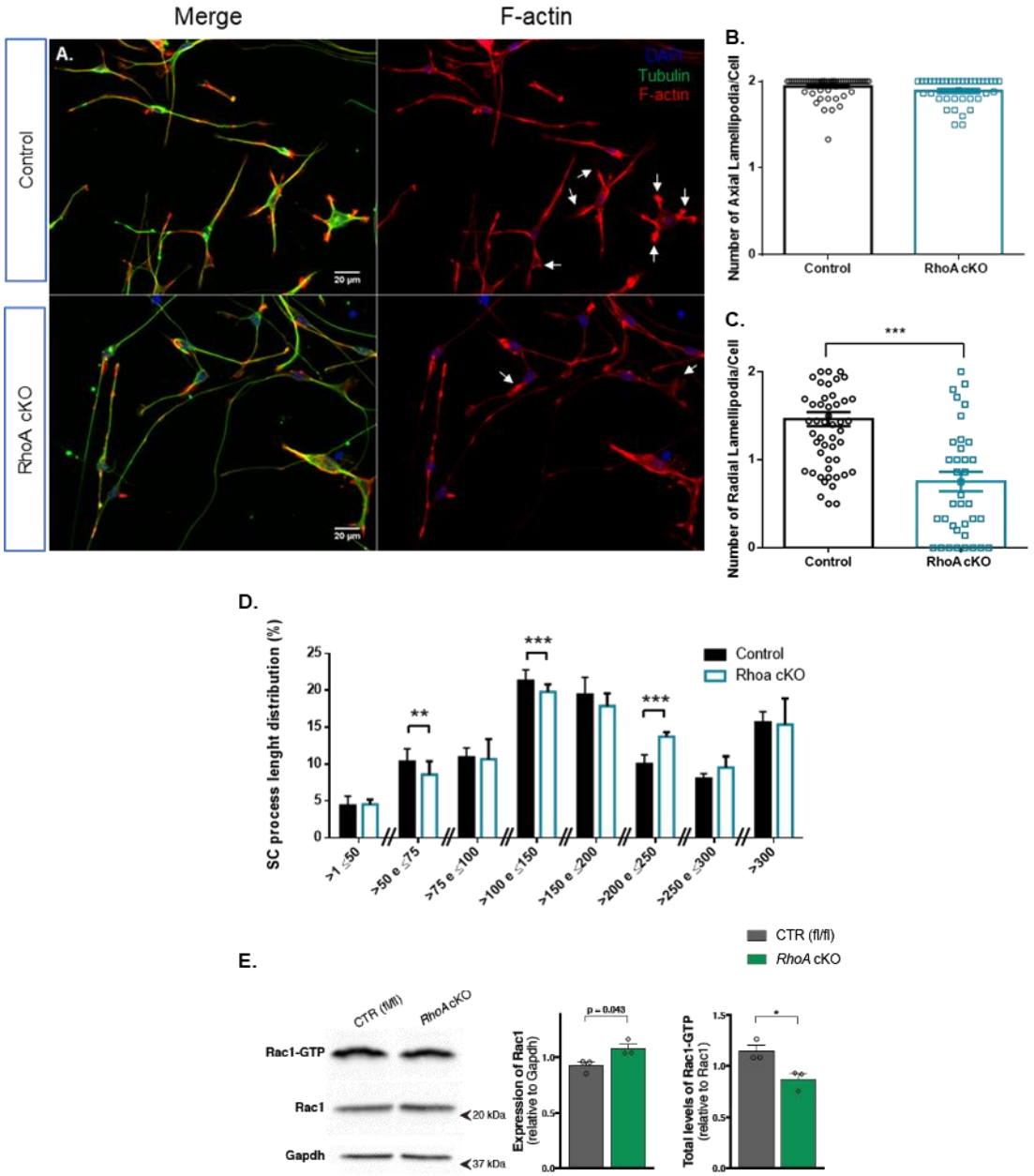


Figure 19 – Process extension is impaired in RhoA cKO SCs. (A) In order to visualize lamellipodia, primary SCs obtained from P4 control and RhoA ckO sciatic nerves were stained with phalloidin (red). The number of axial (B) and radial (C) lamellipodia formed per cell was quantified. (D) The length of axial processes extended by each cell was measured and categorized in intervals. Bars represent the percentage of processes that belong to each interval. Arrows indicate radial lamellipodia. Results were obtained from two independent experiments and pooled together (7 control and 4 RhoA cKO). The number of cells counted was 519 for control and 253 for RhoA cKO.

(E) Pull-down analysis of P5 sciatic nerve lysates and quantification of Rac1 and Rac1-GTP levels. Error bars indicate ± SEM. (*, P <0,05; ***, P <0,001 calculated with Student's *t* test).

2.3. Dysregulation of signalling pathways associated with actin dynamics

The formation of protrusive structures like lamellipodia, as well as process extension requires the assembly of F-actin networks near the plasma membrane. Rho GTPases control actin cytoskeleton dynamics through regulation of several downstream effectors (Spiering et al. 2011). ROCKs are activated by interaction with active Rho (Amano et al. 2010) and certain lipids, like arachidonic acid (Araki et al. 2001). In rats, ROCK1 levels increase gradually from birth through P30 while ROCK2 levels remain relatively stable (Melendez-Vasquez et al. 2004). Rho/ROCK directly phosphorylates profilin (Shao et al. 2008) and indirectly cofilin, through LIMK activation (Ohashi et al. 2000). These two proteins contribute to actin cytoskeleton dynamics in different ways and phosphorylation inactivates them (*Figure 7*). The spatio-temporal control of cofilin activity was previously shown to be essential for proper axon engagement (inactivation) and SC membrane expansion during active myelination (activation) (Sparrow et al. 2012). Previous studies have demonstrated profilin's importance in PNS development. SC specific ablation of profilin resulted in radial sorting defects and hypomyelination. This was attributed to SCs failing to progress from pro-myelinating SCs to myelinating SCs (Montani et al. 2014). The same study also found that profilin activity is essential for radial lamellipodia formation and that its regulation is independent of Rac1 activity and dependent of Rho/ROCK signalling (*Figure 12*).

RhoE (or Rnd3) is an atypical Rho GTPase that interacts with p190RhoGAP, increasing its activity, thereby reducing RhoA-GTP levels (Wennerberg et al. 2003). Also, RhoE is regulated by ROCK 1 mediated phosphorylation (Riento et al. 2005) and can also directly bind to ROCK1, inhibiting downstream signalling (Riento et al. 2003).

In an effort to understand what signalling pathways related with actin cytoskeleton dynamics are deregulated in RhoA ckO, Western-blot analysis of P5 sciatic nerve lysates was performed to assess expression of selected downstream targets (*Figure 20*).

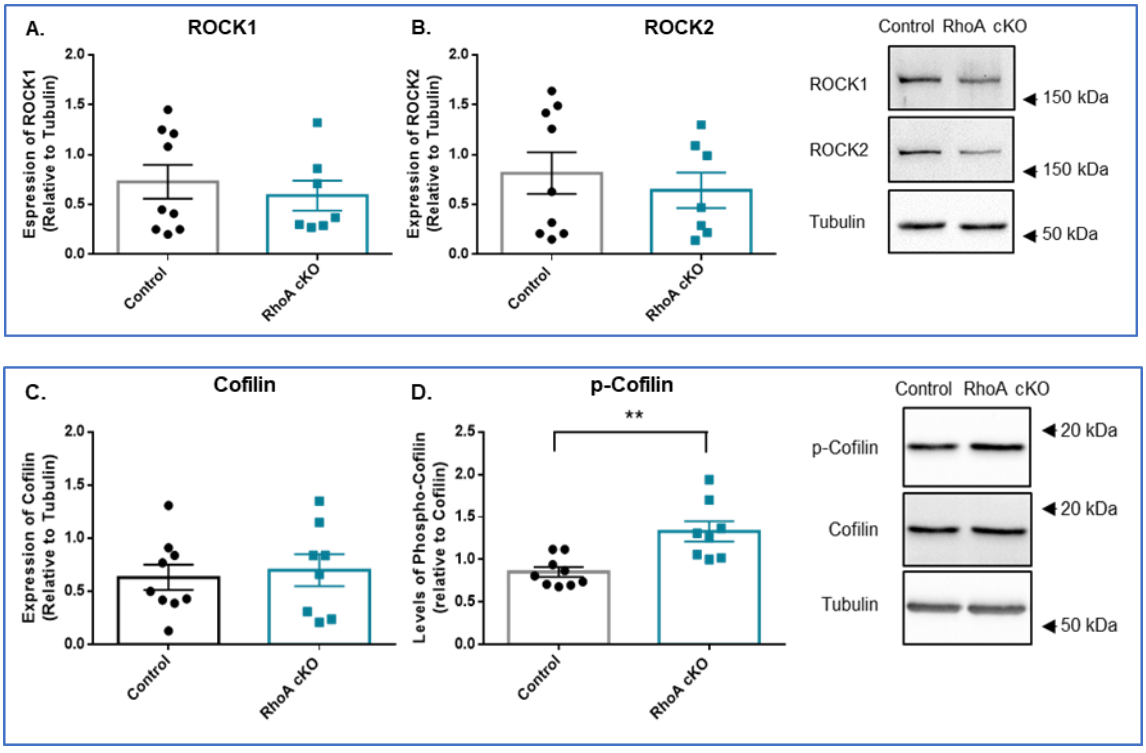
The expression levels of both ROCK1 (*Figure 20A*) and ROCK2 (*Figure 20B*), were found to not altered in mutant sciatic nerves. However, this is an indirect analysis since ROCK activity depends on its direct interaction with Rho (RhoA, B or C) and possibly (auto)phosphorylation (Maekawa et al. 1999). Additionally, RhoE expression levels were also not significantly changed (*Figure 20G*).

Both expression and phosphorylation levels of the actin-binding proteins cofilin and profilin were assessed. Results show that expression levels of these two proteins were not altered in mutants. However, levels of p-cofilin increased in mutant SCs (*Figure 20D*). This was an unexpected result, as cofilin phosphorylation is induced by Rho/ROCK

signalling. However, other Rho GTPases, namely Cdc42, acts through the same signalling pathways (LIMK2) to induce cofilin phosphorylation (Edwards et al. 1999). Additionally, the control of cofilin phosphorylation/dephosphorylation is tightly regulated by a crosstalk between an intricate network of proteins (Mizuno 2013). Taking this into consideration, it is possible that the absence of RhoA either disrupted this regulation, or Cdc42 signalling overcompensated the absence of RhoA leading to increased phosphorylation of cofilin.

Another possible explanation is that the radial sorting and/or onset of myelination delay is the cause and not a consequence of increased cofilin phosphorylation at P5. As proposed by Sparrow et al. (Sparrow et al. 2012), during axon engagement and SC alignment, cofilin inactivation allows for the stabilization of F-actin, while during active myelination, cofilin is activated to allow SC membrane expansion and wrapping around the axon (*Figure 12*). This cofilin dephosphorylation was shown to be axon dependent. Morphometric analyses at P5 has already shown that RhoA-null SCs engage and sort less axons when compared to control (*Figure 13F*). Thus, the increase in phosphorylated cofilin in RhoA cKO could be attributed to reduced NRG1/ErbB signalling.

In contrast, levels of phospho-profilin (*Figure 20 F*) were not significantly altered in mutants. As previous studies showed that profilin phosphorylation is mediated by and dependent on Rho/ROCK signalling in SCs, a possible explanation for these results is that there are other Rho GTPases compensating the absence of RhoA. Indeed, pull-down analysis showed that levels of activated RhoC increased in mutant sciatic nerves, with total levels of the protein showing a strong tendency to increase (p=0.06; *Figure 21*).



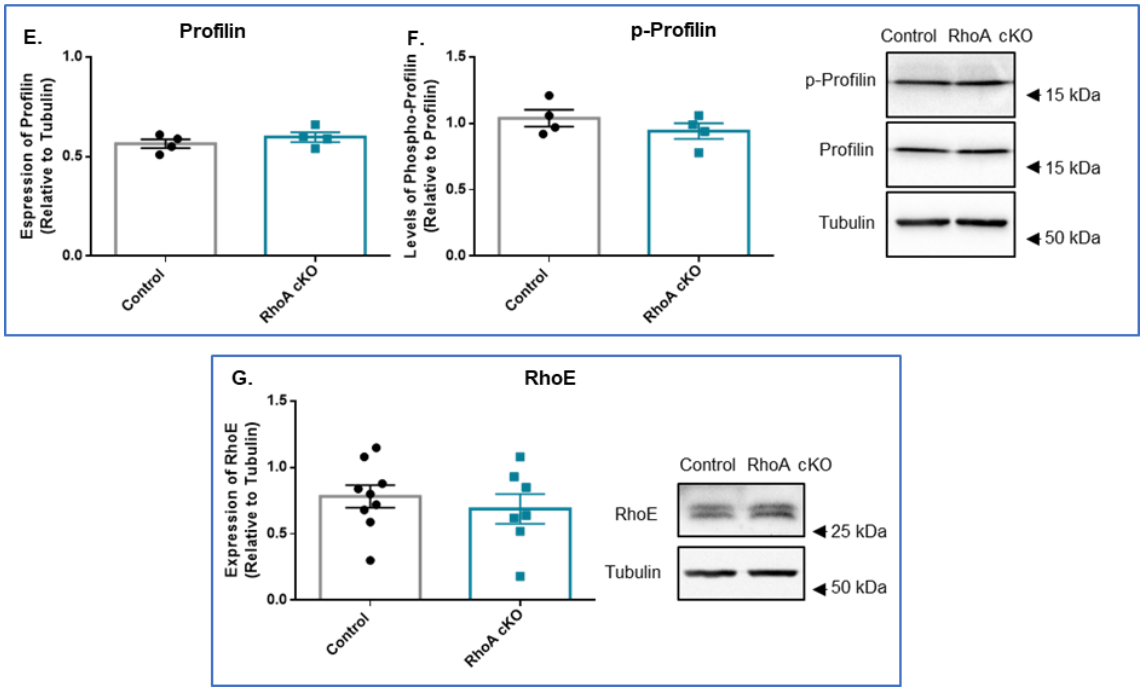


Figure 20 – Western blot analysis of signalling pathways related to actin dynamics. Sciatic nerve lysates obtained from P5 control and RhoA cKO littermates were analysed by Western blot. ROCK1 (A), ROCK2 (B), cofilin (C), profilin (E) and RhoE (G) levels were quantified relative to tubulin (loading control). Levels of the phosphorylated forms of cofilin (D) and profilin (F) are relative to total levels of cofilin and profilin, respectively. Error bars indicate ± SEM. **, P <0,01 calculated with Student's t test.

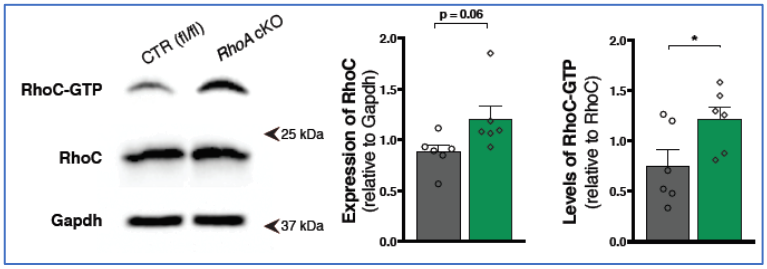


Figure 21 – Pull-down analysis of P5 sciatic nerve lysates and quantification of RhoC and RhoC-GTP levels. Error bars indicate ± SEM. *, P <0,05 calculated with Student's t test.

3. Analysis of myelination

Previous morphometric analyses of sciatic nerves from P15 and P25 RhoA cKO showed that myelin thickness is reduced, suggesting an hypomyelination phenotype (*Figure 15*). A recent study in which RhoA knockdown was accomplished by microinjection of P3 sciatic nerves with RhoA-shRNA lentivirus showed that, after four weeks, myelin thickness and MBP levels assessed by immunohistochemistry were found to be significantly decreased in transfected SCs (Wen et al. 2017). Thus, next we aimed to perform complementary biochemical analyses of sciatic nerves from our RhoA cKO and assess if signalling pathways related to myelination are altered.

3.1. Analysis of internode length and myelin protein levels

The positive correlation between internode length and axon diameter is known since 1875 (Key et al. 1875) and radial growth of axons is dependent upon myelination (de Waegh et al. 1992). Therefore, the state of the myelination process can be indirectly inferred through internode length measurement.

To measure internode length, individual nerve segments obtained from teased sciatic nerves from P25 animals were labelled with a Caspr specific antibody (*Figure 22A*). Caspr is a membrane protein expressed by neurons that concentrates in the paranodal region of the axon (Einheber et al. 1997). Results show that mutants produce significantly shorter internodes when compared with controls (*Figure 22B*). These results are in agreement with previous *in vitro* studies where it was observed that pharmacological inhibition of ROCK resulted in shorter myelin segments being produced by cultured SCs. This observation was attributed to individual SCs organizing up to 4 distinct nodal-paranodal domains, which logically results in shorter internodes (Melendez-Vasquez et al. 2004). In fact, SCs have an important role in organizing membrane proteins and channel clustering in axons (Susuki et al. 2008). Proper formation of paranodal/nodal regions in the PNS is dependent on SC (axial) polarization and formation of microvilli enriched in activated ERM proteins (ezrin, radizin and moesin) that link the actin cytoskeleton to various membrane proteins (Ramesh 2004). These proteins are activated by ROCK mediated phosphorylation (Matsui et al. 1998), which in turn is Rho dependent (Gatto et al. 2003). Therefore, the observed decrease in internode length in mutants could be attributed to deficient formation of nodal/paranodal regions. Short internodes are a pathological hallmark of peripheral neuropathies (Saporta et al. 2009) and are linked to slower conduction velocities of nerve impulses (Court et al. 2004).

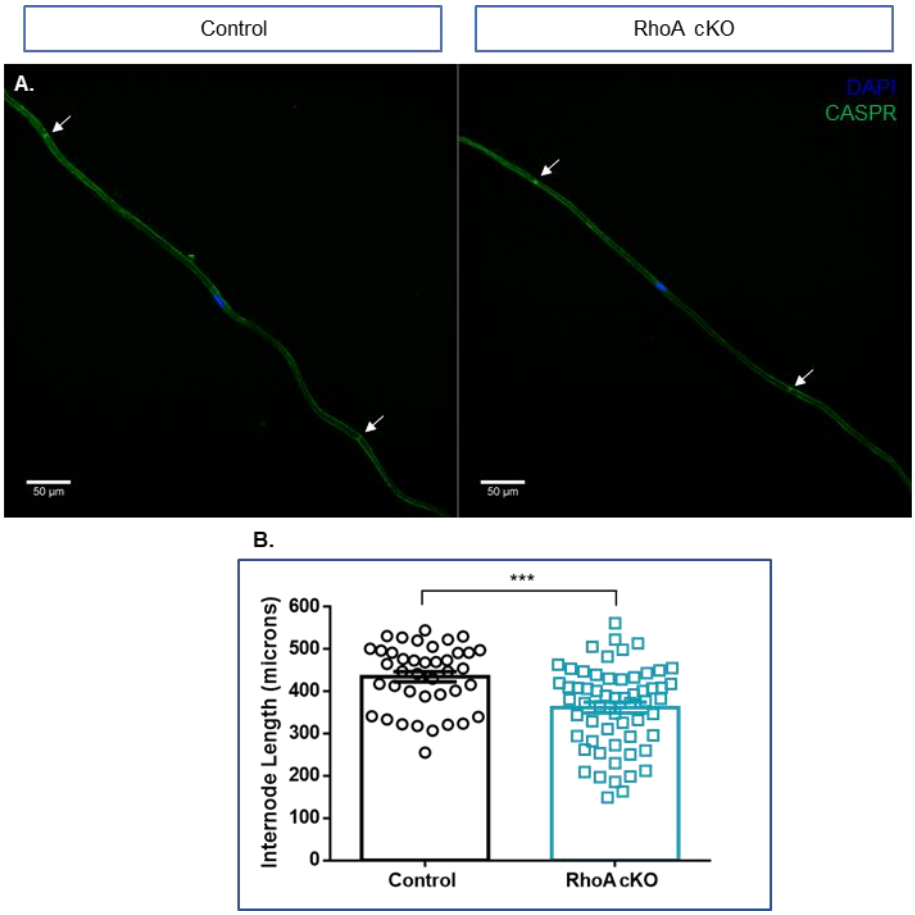


Figure 22 – Internodal length is decreased in RhoA ckO. (A) Teased fibres from P25 control and RhoA cKO sciatic nerves stained with DAPI and CASPR. (B) Individual measurements from 6 control (n=40) and 5 RhoA cKO (n=59) animals were pooled together. Error bars indicate ± SEM. ***, P <0,001 calculated with Student's t test.

In order to perform a complementary analysis of myelin production, Western blot of P15 and P25 sciatic nerve lysates was performed and the relative levels of MBP, a major protein constituent of the myelin sheath, were determined (*Figure 23*). At P15, the levels of MBP were not significantly different between mutants and controls (*Figure 23A*). At P25 however, MBP levels were significantly decreased in mutant lysates, suggesting that sciatic nerves of RhoA cKO are hypomyelinated (*Figure 23B*). MBP levels only being altered at P25 and not at P15 could be attributed to problems with myelin compaction, since MBP is important for this process (Garbay et al. 2000). Therefore, assessing the levels of other myelin proteins, like for example P0 is essential to complete this analysis.

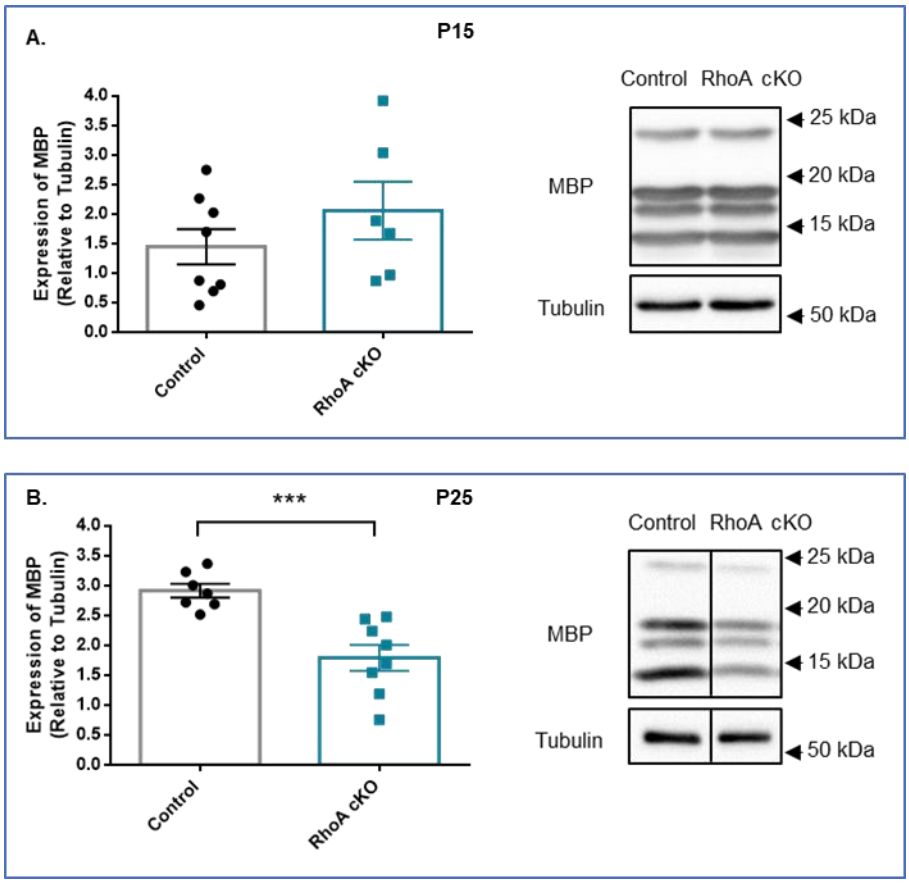


Figure 23 – MBP levels are reduced in RhoA cKO at P25. Western blot analysis of sciatic nerve lysates obtained from (A) P15 and (B) P25 control and RhoA cKO littermates shows a decrease in MBP levels. Error bars indicate ± SEM. ***, P <0,001 calculated with Student's t test.

3.2. Signalling pathways that regulate myelin in the PNS

The PI3K/Akt pathway has been implicated in the control of SC wrapping and myelination via multiple pathways involving, among others, mTOR and Rac1 activation (Domenech-Estevez et al. 2016). Activation of PI3K by axonal Nrg1 type III results in phosphorylation of Akt in two residues: threonine 308 and serine 473. Although phosphorylation of both residues is required for maximal activation of Akt (Manning et al. 2017), phosphorylation of threonine 308 is sufficient for robust Akt activation (Balasuriya et al. 2018). Furthermore, phosphorylation of serine 473 seems to be dependent on activation of β1 integrin by the extracellular matrix. ILK (integrin-linked kinase) is the kinase responsible for this phosphorylation (Pereira et al. 2009). Persistent Akt activation causes hypermyelination in the PNS, indicating that this serine-threonine kinase is a key regulator of this process (Domenech-Estevez et al. 2016).

Therefore, to assess the state of myelination we decided to measure the total levels of Akt, as well as of the individual phosphorylated forms. This was performed by Western blot analysis of P15 sciatic nerve lysates, since active myelination peaks at this stage of development. Results show that these levels were not significantly altered in mutants

(*Figure 24*). Further experiments at P25 are required to assess if the reduction in MBP observed is AKT-dependent.

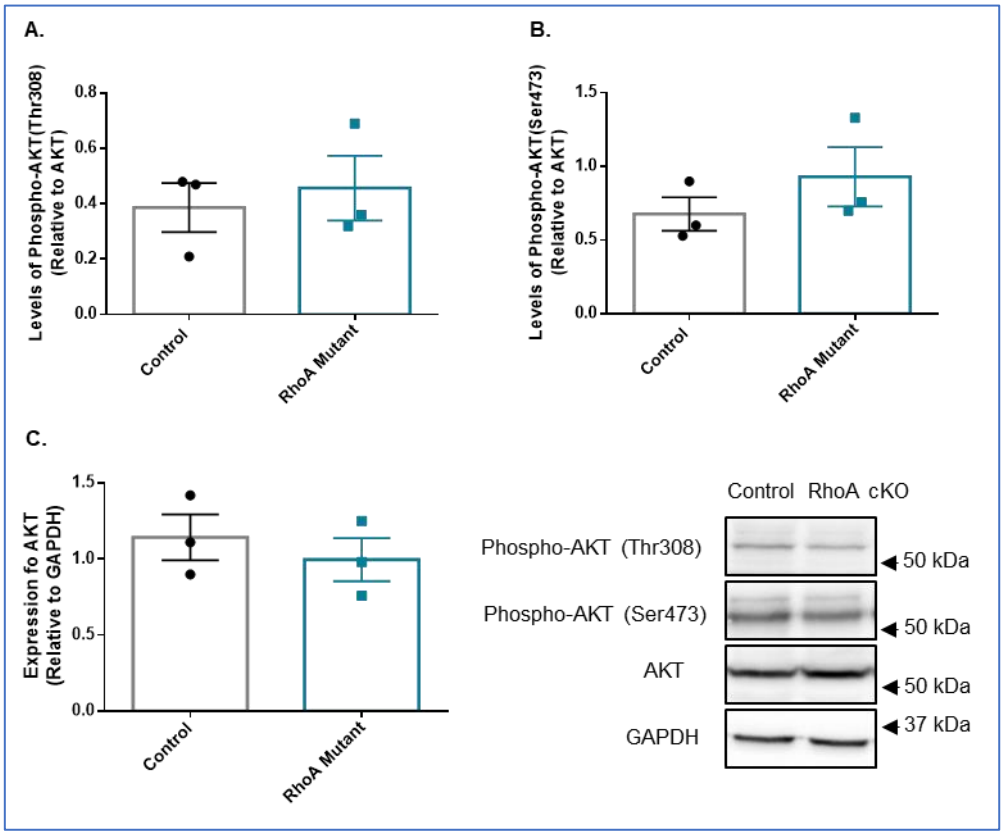


Figure 24 – Western blot analysis of sciatic nerve lysates from control and RhoA cKO littermates at P15 shows that levels of phosphorylated Akt at Thr308 (A), Ser473 (B) and total levels (C) are not significantly altered. Error bars indicate ± SEM.

Chapter IV: Conclusion and future perspectives

In the early postnatal period during developmental myelination in the PNS, SCs extend processes into immature axon bundles, recognising and segregating larger axons (that preferentially get myelinated) to the periphery in a process called radial sorting (Feltri et al. 2016). This process requires a precise spatio-temporal control of SC differentiation, proliferation, survival and dynamic control of the actin cytoskeleton for the formation of specialized cellular protrusions. Rho GTPases act as molecular switches that control actin cytoskeleton dynamics, among other cellular processes (Ridley 2006). Roles for Rac1 and Cdc42 in PNS myelination have been reported. Control of Rac1 activity by β1 integrin signalling in SCs is important for the formation of axial and/or radial lamellipodia depending on the developmental stage (Benninger et al. 2007; Nodari et al. 2007). Furthermore, inhibition of Rho/ROCK signalling is required for SC process extension (Pereira et al. 2009; Montani et al. 2014), while RhoA activation via GPR56 appears to control SC adhesion to axons during axon engagement (Ackerman et al. 2018). On the other hand, Cdc42 is important for SC proliferation (Benninger et al. 2007). In this work we used a conditional knockout mouse model to study the role of RhoA in SC biology and PNS developmental myelination.

Previously performed morphometric analysis of sciatic nerves from RhoA ckO mice in the early post-natal stage showed that there is a delay in radial sorting and onset of myelination (*Figure 13*). This could be attributed to an impairment in SC differentiation, proliferation, survival or cytoskeletal defects. Quantitative real-time PCR analysis to assess expression levels of several differentiation markers suggests that there is no impairment in SC differentiation in the absence of RhoA (*Figure 14*).

In this work, analysis by TUNEL assay suggested that SC survival is not affected in RhoA cKO sciatic nerves (*Figure 18*). Next, we decided to explore the hypothesis that actin cytoskeleton dynamics is deregulated when RhoA is ablated. Using primary SCs isolated from control and mutant sciatic nerves, we found that SCs obtained from RhoA cKO sciatic nerves extend less radial membrane protrusions (lamellipodia) per cell (*Figure 19C*). We also found that mutant SCs extend longer axial processes (*Figure 19D*), suggesting an impairment in the transition of SCs between migration/elongation along axons and axon segregation/wrapping that could contribute to observed impairment in radial sorting and onset of myelination. These results also confirm previous reports that Rho/ROCK activity regulates process length in SCs (Pereira et al. 2009). Exploring what downstream signalling pathways are involved in this deregulation was the next step in this project.

ROCK is enzymatically inactive in its native form, due to auto-inhibition by its carboxyl-terminal region (Jacobs et al. 2006) and it is activated by interaction with active Rho (Amano et al. 2010). Pharmacological inhibition of ROCK re-established radial sorting in *ILK* cKO sciatic nerves, where Rho (RhoA, B and C) activity was increased (Pereira et al. 2009). Western blot analysis of ROCK1 and ROCK2 showed that the expression levels of both kinases were unchanged in RhoA mutant sciatic nerves (*Figure 20A and B*), but because ROCK activity mainly depends on Rho GTPase binding, alternative techniques, such as using a commercial ROCK activity assay kit, should be used in the future. Levels of the atypical Rho GTPase RhoE were also not altered (*Figure 20G*).

Spatio/temporal regulation of cofilin activity by NRG1/ErbB signalling is important in SC myelination (Sparrow et al. 2012). This activity is controlled by Rac1/Cdc42/PAK (Edwards et al. 1999) and Rho/ROCK (Ohashi et al. 2000) signalling (*Figure 12*). Western-blot analysis showed that phosphorylation of cofilin is increased in RhoA mutant sciatic nerves (*Figure 20D*). This could be attributed either to increased Cdc42 activity or compensation by other proteins of the RhoA subfamily. Pull-down analysis showed that active RhoC levels, a Rho GTPase that is very similar to RhoA, (Wheeler et al. 2004) and has higher affinity to ROCK1 and ROCK2 (*Table 3*), are increased in RhoA mutants (*Figure 21*). Injection of RhoA cKO sciatic nerves with Fasudil, a potent ROCK inhibitor, could help clarify this. This deregulation could also be a consequence, and not the cause of the radial sorting delay observed, since axon dependent signalling through NRG1/ErbB was shown to induce cofilin dephosphorylation during active myelination (Sparrow et al. 2012). Upon NRG binding, ErbB undergoes hetero/homodimerization and conformational changes that lead to autophosphorylation. Also, ErbB2 is the preferred heterodimerization partner of all other ErbB family members (Garrett et al. 2003). For these reasons, quantification of phosphorylated and total ErBb2 levels is a good approach to assess if NRG1/ErbB signalling is reduced in RhoA cKO at P5. Nevertheless, increased levels of phospho-cofilin could explain the reduction in radial lamellipodia number observed in cultured RhoA-null SCs. Assessing whether inhibition of cofilin phosphorylation by pharmaceutical inhibitors restores normal numbers of radial lamellipodia is a good strategy to elucidate this question.

Profilin is another actin binding protein that is regulated by Rho/ROCK mediated phosphorylation (Shao et al. 2008). Previous studies showed that SC specific ablation of profilin resulted in radial sorting defects and hypomyelination and that profilin activity is essential for radial lamellipodia formation (Montani et al. 2014). Levels of phospho-profilin were not altered in RhoA mutants (*Figure 20F*), suggesting once again compensation by RhoC.

RhoA knockdown in P3 sciatic nerves resulted in reduction of myelin thickness and MBP signal in transfected SCs after four weeks (Wen et al. 2017). Previous morphometric analysis of later stages of myelination also showed a reduction in myelin thickness (*Figure 15*). In this work, analysis of the state of myelination in older (P15 and P25) mice was performed by two methods: measurement of internode length and biochemical analysis. In mutant P25 sciatic nerves, internodes were found to be shorter (*Figure 22*) which possibly indicates a reduction in myelin production. However, this could also be attributed to abnormal organization of the nodal/paranodal regions, as previously reported (Melendez-Vasquez et al. 2004). In the future, it would be interesting to analyse the distribution of nodal/paranodal proteins in mutants, such as voltage-gated sodium channels or ankyrin G using, for example immunofluorescence techniques, in order to evaluate if the reduction in internodal length is attributed to abnormal formation of these regions. EM analysis of nodal/paranodal regions would also be helpful to understand this. Western blot analysis showed that MBP levels were reduced at P25 (*Figure 23B*), but not at P15 (*Figure 23A*). No differences being observed at P15 could be attributed to the fact that at earlier stages of development the differences in MBP levels cannot be detected by Western blot analysis or are only detectable when myelination is complete and compaction has occurred (P25).

Control of SC membrane wrapping and myelination has previously been shown to be dependent on the PI3K/Akt pathway, since persistent Akt activation causes hypermyelination in the PNS (Domenech-Estevez et al. 2016). Levels of Akt were analysed at P15 (*Figure 24*) and no differences were observed between controls and mutants, suggesting that, in this timepoint, this pathway is not associated with the hypomyelination phenotype. However, analysis of later timepoints is necessary to understand if the reduction in MBP levels and decrease in myelin thickness observed at P25 is AKT dependent.

Overall, these results provide a connection between the radial sorting defects previously observed when RhoA is ablated from SCs and deregulation of the control of actin cytoskeleton dynamics, although additional studies are necessary to investigate if defects in SC proliferation also contribute to this phenotype.

Pharmacological inhibition of the Rho/ROCK pathway is a promising strategy being explored in the treatment of various neurological disorders of the CNS, including spinal cord injury, Alzheimer's, neuropathic pain and demyelinating diseases like multiple sclerosis (Mueller et al. 2005). In fact, various studies found that expression levels of ROCKs are increased in human nervous tissue under pathological conditions, particularly in neurodegenerative disorders. Roles for ROCKs in biological processes linked to these diseases, like neurite outgrowth and regeneration, neuronal survival and

synaptogenesis have been elucidated, particularly in the last decade (Koch et al. 2018). Currently, only two ROCK inhibitors, fasudil (Eril®) and its derivative ripasudil (Glanatec®), have been licenced for clinical use (Koch et al. 2018) (Garnock-Jones 2014). Current ROCK inhibitors also act on other protein kinases (Davies et al. 2000) making the point that some of the beneficial effects are attributed to inhibition of other molecules than ROCK. Further exploration of the role of RhoA in PNS myelination and remyelination could contribute for the assessment of possible side effects of ROCK inhibitor applications in the clinic. Therefore, it constitutes an important task for the future and will provide a better understanding of nerve biology in health and disease.

Chapter V: References

Ackerman, Sarah D., Rong Luo, Yannick Poitelon, Amit Mogha, Breanne L. Harty, Mitchell D'Rozario, Nicholas E. Sanchez, Asvin K.K. Lakkaraju, Paul Gamble, Jun Li, Jun Qu, Matthew R. MacEwan, Wilson Zachary Ray, Adriano Aguzzi, M. Laura Feltri, Xianhua Piao, and Kelly R. Monk. 2018. 'GPR56/ADGRG1 regulates development and maintenance of peripheral myelin', *J Exp Med*.

Adamson, P., H. F. Paterson, and A. Hall. 1992. 'Intracellular localization of the P21rho proteins', *J Cell Biol*, 119: 617-27.

Alberts, B., J.H. Wilson, A. Johnson, T. Hunt, J. Lewis, M. Raff, K. Roberts, and P. Walter. 2008. *Molecular Biology of the Cell: Reference edition* (Garland Science).

Amano, M., M. Ito, K. Kimura, Y. Fukata, K. Chihara, T. Nakano, Y. Matsuura, and K. Kaibuchi. 1996. 'Phosphorylation and activation of myosin by Rho-associated kinase (Rho-kinase)', *J Biol Chem*, 271: 20246-9.

Amano, Mutsuki, Masanori Nakayama, and Kozo Kaibuchi. 2010. 'Rho-Kinase/ROCK: A Key Regulator of the Cytoskeleton and Cell Polarity', *Cytoskeleton (Hoboken, N.j.)*, 67: 545-54.

Aquino, Jorge B., Jens Hjerling-Leffler, Martin Koltzenburg, Thomas Edlund, Marcelo J. Villar, and Patrik Ernfors. 2006. 'In vitro and in vivo differentiation of boundary cap neural crest stem cells into mature Schwann cells', *Experimental Neurology*, 198: 438-49.

Araki, S., M. Ito, Y. Kureishi, J. Feng, H. Machida, N. Isaka, M. Amano, K. Kaibuchi, D. J. Hartshorne, and T. Nakano. 2001. 'Arachidonic acid-induced Ca2+ sensitization of smooth muscle contraction through activation of Rho-kinase', *Pflugers Arch*, 441: 596-603.

Arroyo, E. J., J. R. Bermingham, Jr., M. G. Rosenfeld, and S. S. Scherer. 1998. 'Promyelinating Schwann cells express Tst-1/SCIP/Oct-6', *J Neurosci*, 18: 7891-902.

Balasuriya, N., M. T. Kunkel, X. Liu, K. K. Biggar, S. S. Li, A. C. Newton, and P. O'Donoghue. 2018. 'Genetic code expansion and live cell imaging reveal that Thr-308 phosphorylation is irreplaceable and sufficient for Akt1 activity', *J Biol Chem*, 293: 10744-56.

Barker, Alison J., and Erik M. Ullian. 2008. 'New roles for astrocytes in developing synaptic circuits', *Communicative & Integrative Biology*, 1: 207-11.

Ben Geren, B. 1954. 'The formation from the Schwann cell surface of myelin in the peripheral nerves of chick embryos', *Exp Cell Res*, 7: 558-62.

Benninger, Y., T. Thurnherr, J. A. Pereira, S. Krause, X. Wu, A. Chrostek-Grashoff, D. Herzog, K. A. Nave, R. J. Franklin, D. Meijer, C. Brakebusch, U. Suter, and J. B. Relvas. 2007. 'Essential and distinct roles for cdc42 and rac1 in the regulation of Schwann cell biology during peripheral nervous system development', *J Cell Biol*, 177: 1051-61.

Berti, C., L. Bartesaghi, M. Ghidinelli, D. Zambroni, G. Figlia, Z. L. Chen, A. Quattrini, L. Wrabetz, and M. L. Feltri. 2011. 'Non-redundant function of dystroglycan and beta1 integrins in radial sorting of axons', *Development*, 138: 4025-37.

Britsch, S., D. E. Goerich, D. Riethmacher, R. I. Peirano, M. Rossner, K. A. Nave, C. Birchmeier, and M. Wegner. 2001. 'The transcription factor Sox10 is a key regulator of peripheral glial development', *Genes Dev*, 15: 66-78.

Bustelo, X. R., V. Sauzeau, and I. M. Berenjeno. 2007. 'GTP-binding proteins of the Rho/Rac family: regulation, effectors and functions in vivo', *Bioessays*, 29: 356-70.

Catala, M., and N. Kubis. 2013. 'Gross anatomy and development of the peripheral nervous system', *Handb Clin Neurol*, 115: 29-41.

Chen, Z. L., and S. Strickland. 2003. 'Laminin gamma1 is critical for Schwann cell differentiation, axon myelination, and regeneration in the peripheral nerve', *J Cell Biol*, 163: 889-99.

Chen, Zu-Lin, Wei-Ming Yu, and Sidney Strickland. 2007. 'Peripheral Regeneration', *Annu Rev Neurosci*, 30: 209-33.

Court, F. A., D. L. Sherman, T. Pratt, E. M. Garry, R. R. Ribchester, D. F. Cottrell, S. M. Fleetwood-Walker, and P. J. Brophy. 2004. 'Restricted growth of Schwann cells lacking Cajal bands slows conduction in myelinated nerves', *Nature*, 431: 191-5.

Davies, S. P., H. Reddy, M. Caivano, and P. Cohen. 2000. 'Specificity and mechanism of action of some commonly used protein kinase inhibitors', *Biochem J*, 351: 95-105.

De La Cruz, Enrique M. 2009. 'How cofilin severs an actin filament', *Biophysical Reviews*, 1: 51-59.

de Waegh, Sylvie M., Virginia M. Y. Lee, and Scott T. Brady. 1992. 'Local modulation of neurofilament phosphorylation, axonal caliber, and slow axonal transport by myelinating Schwann cells', *Cell*, 68: 451-63.

Decker, L., C. Desmarquet-Trin-Dinh, E. Taillebourg, J. Ghislain, J. M. Vallat, and P. Charnay. 2006. 'Peripheral myelin maintenance is a dynamic process requiring constant Krox20 expression', *J Neurosci*, 26: 9771-9.

Domenech-Estevez, E., H. Baloui, X. Meng, Y. Zhang, K. Deinhardt, J. L. Dupree, S. Einheber, R. Chrast, and J. L. Salzer. 2016. 'Akt Regulates Axon Wrapping and Myelin Sheath Thickness in the PNS', *J Neurosci*, 36: 4506-21.

Echelard, Y., D. J. Epstein, B. St-Jacques, L. Shen, J. Mohler, J. A. McMahon, and A. P. McMahon. 1993. 'Sonic hedgehog, a member of a family of putative signaling molecules, is implicated in the regulation of CNS polarity', *Cell*, 75: 1417-30.

Edwards, D. C., L. C. Sanders, G. M. Bokoch, and G. N. Gill. 1999. 'Activation of LIM-kinase by Pak1 couples Rac/Cdc42 GTPase signalling to actin cytoskeletal dynamics', *Nat Cell Biol*, 1: 253-9.

Einheber, S., G. Zanazzi, W. Ching, S. Scherer, T. A. Milner, E. Peles, and J. L. Salzer. 1997. 'The axonal membrane protein Caspr, a homologue of neurexin IV, is a component of the septate-like paranodal junctions that assemble during myelination', *J Cell Biol*, 139: 1495-506.

Etienne-Manneville, S., and A. Hall. 2002. 'Rho GTPases in cell biology', *Nature*, 420: 629-35.

Fawcett, J. W., and R. J. Keynes. 1990. 'Peripheral nerve regeneration', *Annu Rev Neurosci*, 13: 43-60.

Feltri, M. L., D. Graus Porta, S. C. Previtali, A. Nodari, B. Migliavacca, A. Cassetti, A. Littlewood-Evans, L. F. Reichardt, A. Messing, A. Quattrini, U. Mueller, and L. Wrabetz. 2002. 'Conditional disruption of beta 1 integrin in Schwann cells impedes interactions with axons', *J Cell Biol*, 156: 199-209.

Feltri, M. L., Y. Poitelon, and S. C. Previtali. 2016. 'How Schwann Cells Sort Axons: New Concepts', *Neuroscientist*, 22: 252-65.

Friede Reinhard, L. 1972. 'Control of myelin formation by axon caliber. (With a model of the control mechanism)', *Journal of Comparative Neurology*, 144: 233-52.

Garbay, B., A. M. Heape, F. Sargueil, and C. Cassagne. 2000. 'Myelin synthesis in the peripheral nervous system', *Progress in Neurobiology*, 61: 267-304.

Garnock-Jones, K. P. 2014. 'Ripasudil: first global approval', *Drugs*, 74: 2211-5.

Garratt, A. N., S. Britsch, and C. Birchmeier. 2000. 'Neuregulin, a factor with many functions in the life of a schwann cell', *Bioessays*, 22: 987-96.

Garrett, T. P., N. M. McKern, M. Lou, T. C. Elleman, T. E. Adams, G. O. Lovrecz, M. Kofler, R. N. Jorissen, E. C. Nice, A. W. Burgess, and C. W. Ward. 2003. 'The crystal structure of a truncated ErbB2 ectodomain reveals an active conformation, poised to interact with other ErbB receptors', *Mol Cell*, 11: 495-505.

Gatto, Cheryl L., Barbara J. Walker, and Stephen Lambert. 2003. 'Local ERM activation and dynamic growth cones at Schwann cell tips implicated in efficient formation of nodes of Ranvier', *J Cell Biol*, 162: 489-98.

Gavrieli, Y., Y. Sherman, and S. A. Ben-Sasson. 1992. 'Identification of programmed cell death in situ via specific labeling of nuclear DNA fragmentation', *J Cell Biol*, 119: 493-501.

Ghislain, Julien, Carole Desmarquet-Trin-Dinh, Martine Jaegle, Dies Meijer, Patrick Charnay, and Monique Frain. 2002. 'Characterisation of cis-acting sequences reveals a biphasic, axon-dependent regulation of Krox20 during Schwann cell development', *Development*, 129: 155-66.

Giaume, C., F. Kirchhoff, C. Matute, A. Reichenbach, and A. Verkhratsky. 2007. 'Glia: the fulcrum of brain diseases', *Cell Death Differ*, 14: 1324-35.

Goebbels, S., J. H. Oltrogge, R. Kemper, I. Heilmann, I. Bormuth, S. Wolfer, S. P. Wichert, W. Mobius, X. Liu, C. Lappe-Siefke, M. J. Rossner, M. Groszer, U. Suter, J. Frahm, S. Boretius, and K. A. Nave. 2010. 'Elevated phosphatidylinositol 3,4,5-trisphosphate in glia triggers cell-autonomous membrane wrapping and myelination', *J Neurosci*, 30: 8953-64.

Goldschmidt-Clermont, P. J., M. I. Furman, D. Wachsstock, D. Safer, V. T. Nachmias, and T. D. Pollard. 1992. 'The control of actin nucleotide exchange by thymosin beta 4 and profilin. A potential regulatory mechanism for actin polymerization in cells', *Molecular Biology of the Cell*, 3: 1015-24.

Grigoryan, T., S. Stein, J. Qi, H. Wende, A. N. Garratt, K. A. Nave, C. Birchmeier, and W. Birchmeier. 2013. 'Wnt/Rspondin/beta-catenin signals control axonal sorting and lineage progression in Schwann cell development', *Proc Natl Acad Sci U S A*, 110: 18174-9.

Grove, M., N. H. Komiyama, K. A. Nave, S. G. Grant, D. L. Sherman, and P. J. Brophy. 2007. 'FAK is required for axonal sorting by Schwann cells', *J Cell Biol*, 176: 277-82.

Guilluy, Christophe, Rafael Garcia-Mata, and Keith Burridge. 2011. 'Rho protein crosstalk: another social network?', *Trends in Cell Biology*, 21: 718-26.

Hall, A. 1998. 'Rho GTPases and the actin cytoskeleton', *Science*, 279: 509-14.

Hanani, Menachem. 2005. 'Satellite glial cells in sensory ganglia: from form to function', *Brain Research Reviews*, 48: 457-76.

Hayasaka, Kiyoshi, Masato Himoro, Wataru Sato, Goro Takada, Keiichi Uyemura, Nobuyoshi Shimizu, Thomas D. Bird, P. Michael Conneally, and Phillip F. Chance. 1993. 'Charcot–Marie–Tooth neuropathy type 1B is associated with mutations of the myelin P0 gene', *Nature Genetics*, 5: 31.

Heasman, S. J., and A. J. Ridley. 2008. 'Mammalian Rho GTPases: new insights into their functions from in vivo studies', *Nat Rev Mol Cell Biol*, 9: 690-701.

Jackson, B., K. Peyrollier, E. Pedersen, A. Basse, R. Karlsson, Z. Wang, T. Lefever, A. M. Ochsenbein, G. Schmidt, K. Aktories, A. Stanley, F. Quondamatteo, M. Ladwein, K. Rottner, J. van Hengel, and C. Brakebusch. 2011. 'RhoA is dispensable for skin development, but crucial for contraction and directed migration of keratinocytes', *Mol Biol Cell*, 22: 593-605.

Jacobs, M., K. Hayakawa, L. Swenson, S. Bellon, M. Fleming, P. Taslimi, and J. Doran. 2006. 'The structure of dimeric ROCK I reveals the mechanism for ligand selectivity', *J Biol Chem*, 281: 260-8.

Jaegle, M., W. Mandemakers, L. Broos, R. Zwart, A. Karis, P. Visser, F. Grosveld, and D. Meijer. 1996. 'The POU factor Oct-6 and Schwann cell differentiation', *Science*, 273: 507-10.

Jagalur, N. B., M. Ghazvini, W. Mandemakers, S. Driegen, A. Maas, E. A. Jones, M. Jaegle, F. Grosveld, J. Svaren, and D. Meijer. 2011. 'Functional dissection of the Oct6 Schwann cell enhancer reveals an essential role for dimeric Sox10 binding', *J Neurosci*, 31: 8585-94.

Jessen, K. R., A. Brennan, L. Morgan, R. Mirsky, A. Kent, Y. Hashimoto, and J. Gavrilovic. 1994. 'The schwann cell precursor and its fate: A study of cell death and differentiation during gliogenesis in rat embryonic nerves', *Neuron*, 12: 509-27.

Jessen, K. R., and R. Mirsky. 2005. 'The origin and development of glial cells in peripheral nerves', *Nat Rev Neurosci*, 6: 671-82.

Jessen, K. R., and R. Mirsky. 2016. 'The repair Schwann cell and its function in regenerating nerves', *J Physiol*, 594: 3521-31.

Kao, S. C., H. Wu, J. Xie, C. P. Chang, J. A. Ranish, I. A. Graef, and G. R. Crabtree. 2009. 'Calcineurin/NFAT signaling is required for neuregulin-regulated Schwann cell differentiation', *Science*, 323: 651-4.

Key, A., and G. Retzius. 1875. 'Studien in der Anatomie des Nervensystems und des Bindegewebe. Samson and Wallin, Stockholm', 2: 228.

Koch, Jan Christoph, Lars Tatenhorst, Anna-Elisa Roser, Kim-Ann Saal, Lars Tönges, and Paul Lingor. 2018. 'ROCK inhibition in models of neurodegeneration and its potential for clinical translation', *Pharmacology & Therapeutics*, 189: 1-21.

Kuhlbrodt, K., B. Herbarth, E. Sock, I. Hermans-Borgmeyer, and M. Wegner. 1998. 'Sox10, a novel transcriptional modulator in glial cells', *J Neurosci*, 18: 237-50.

Lappe-Siefke, Corinna, Sandra Goebbels, Michel Gravel, Eva Nicksch, John Lee, Peter E. Braun, Ian R. Griffiths, and Klaus-Armin Nave. 2003. 'Disruption of Cnp1 uncouples oligodendroglial functions in axonal support and myelination', *Nature Genetics*, 33: 366.

Lee, M. J., A. Brennan, A. Blanchard, G. Zoidl, Z. Dong, A. Tabernero, C. Zoidl, M. A. R. Dent, K. R. Jessen, and R. Mirsky. 1997. 'P0Is Constitutively Expressed in the Rat Neural Crest and Embryonic Nerves and Is Negatively and Positively Regulated by Axons to Generate Non-Myelin-Forming and Myelin-Forming Schwann Cells, Respectively', *Molecular and Cellular Neuroscience*, 8: 336-50.

Leitman, Ellen M., Ambika Tewari, Meryl Horn, Mateusz Urbanski, Evangelos Damanakis, Steven Einheber, James L. Salzer, Primal de Lanerolle, and Carmen V. Melendez-Vasquez. 2011. 'MLCK regulates Schwann cell cytoskeletal organization, differentiation and myelination', *Journal of Cell Science*, 124: 3784-96.

Love, S. 2006. 'Demyelinating diseases', *Journal of Clinical Pathology*, 59: 1151-59.

Maciver, S. K., and A. G. Weeds. 1994. 'Actophorin preferentially binds monomeric ADP-actin over ATP-bound actin: consequences for cell locomotion', *FEBS Lett*, 347: 251-6.

Maekawa, M., T. Ishizaki, S. Boku, N. Watanabe, A. Fujita, A. Iwamatsu, T. Obinata, K. Ohashi, K. Mizuno, and S. Narumiya. 1999. 'Signaling from Rho to the actin cytoskeleton through protein kinases ROCK and LIM-kinase', *Science*, 285: 895-8.

Manning, B. D., and A. Toker. 2017. 'AKT/PKB Signaling: Navigating the Network', *Cell*, 169: 381-405.

Marchionni, M. A., A. D. Goodearl, M. S. Chen, O. Bermingham-McDonogh, C. Kirk, M. Hendricks, F. Danehy, D. Misumi, J. Sudhalter, K. Kobayashi, and et al. 1993. 'Glial growth factors are alternatively spliced erbB2 ligands expressed in the nervous system', *Nature*, 362: 312-8.

Maro, Géraldine S., Matthieu Vermeren, Octavian Voiculescu, Lisa Melton, James Cohen, Patrick Charnay, and Piotr Topilko. 2004. 'Neural crest boundary cap cells constitute a source of neuronal and glial cells of the PNS', *Nature Neuroscience*, 7: 930.

Matsui, T., M. Maeda, Y. Doi, S. Yonemura, M. Amano, K. Kaibuchi, S. Tsukita, and S. Tsukita. 1998. 'Rho-kinase phosphorylates COOH-terminal threonines of ezrin/radixin/moesin (ERM) proteins and regulates their head-to-tail association', *J Cell Biol*, 140: 647-57.

Mayor, Roberto, and Eric Theveneau. 2013. 'The neural crest', *Development*, 140: 2247-51.

Melendez-Vasquez, Carmen V., Steven Einheber, and James L. Salzer. 2004. 'Rho Kinase Regulates Schwann Cell Myelination and Formation of Associated Axonal Domains', *The Journal of Neuroscience*, 24: 3953-63.

Michailov, G. V., M. W. Sereda, B. G. Brinkmann, T. M. Fischer, B. Haug, C. Birchmeier, L. Role, C. Lai, M. H. Schwab, and K. A. Nave. 2004. 'Axonal neuregulin-1 regulates myelin sheath thickness', *Science*, 304: 700-3.

Mizuno, Kensaku. 2013. 'Signaling mechanisms and functional roles of cofilin phosphorylation and dephosphorylation', *Cell Signal*, 25: 457-69.

Monk, K. R., M. L. Feltri, and C. Taveggia. 2015. 'New insights on Schwann cell development', *Glia*, 63: 1376-93.

Montani, Laura, Tina Buerki-Thurnherr, Joana Paes de Faria, Jorge A. Pereira, Nuno G. Dias, Rui Fernandes, Ana F. Gonçalves, Attila Braun, Yves Benninger, Ralph T. Böttcher, Mercedes Costell, Klaus-Armin Nave, Robin J. M. Franklin, Dies Meijer, Ueli Suter, and João B. Relvas. 2014. 'Profilin 1 is required for peripheral nervous system myelination', *Development*, 141: 1553-61.

Moon, S. Y., and Y. Zheng. 2003. 'Rho GTPase-activating proteins in cell regulation', *Trends Cell Biol*, 13: 13-22.

Morrison, Sean J., Sharon E. Perez, Zhou Qiao, Joseph M. Verdi, Carol Hicks, Gerry Weinmaster, and David J. Anderson. 2000. 'Transient Notch Activation Initiates an Irreversible Switch from Neurogenesis to Gliogenesis by Neural Crest Stem Cells', *Cell*, 101: 499-510.

Mueller, B. K., H. Mack, and N. Teusch. 2005. 'Rho kinase, a promising drug target for neurological disorders', *Nat Rev Drug Discov*, 4: 387-98.

Mukhopadhyay, G., P. Doherty, F. S. Walsh, P. R. Crocker, and M. T. Filbin. 1994. 'A novel role for myelin-associated glycoprotein as an inhibitor of axonal regeneration', *Neuron*, 13: 757-67.

Mukouyama, Yoh-suke, Hans-Peter Gerber, Napoleone Ferrara, Chenghua Gu, and David J. Anderson. 2005. 'Peripheral nerve-derived VEGF promotes arterial differentiation via neuropilin 1-mediated positive feedback', *Development*, 132: 941-52.

Newbern, J. M., X. Li, S. E. Shoemaker, J. Zhou, J. Zhong, Y. Wu, D. Bonder, S. Hollenback, G. Coppola, D. H. Geschwind, G. E. Landreth, and W. D. Snider. 2011. 'Specific functions for ERK/MAPK signaling during PNS development', *Neuron*, 69: 91-105.

Nodari, A., D. Zambroni, A. Quattrini, F. A. Court, A. D'Urso, A. Recchia, V. L. Tybulewicz, L. Wrabetz, and M. L. Feltri. 2007. 'Beta1 integrin activates Rac1 in Schwann cells to generate radial lamellae during axonal sorting and myelination', *J Cell Biol*, 177: 1063-75.

Norton, W. T., and Wendy Cammer. 1984. *Isolation and Characterization of Myelin*.

Novak, Nurit, Vered Bar, Helena Sabanay, Shahar Frechter, Martine Jaegle, Scott B. Snapper, Dies Meijer, and Elior Peles. 2011. 'N-WASP is required for membrane wrapping and myelination by Schwann cells', *J Cell Biol*, 192: 243-50.

Ohashi, K., K. Nagata, M. Maekawa, T. Ishizaki, S. Narumiya, and K. Mizuno. 2000. 'Rho-associated kinase ROCK activates LIM-kinase 1 by phosphorylation at threonine 508 within the activation loop', *J Biol Chem*, 275: 3577-82.

Olofsson, B. 1999. 'Rho guanine dissociation inhibitors: pivotal molecules in cellular signalling', *Cell Signal*, 11: 545-54.

Parmantier, E., B. Lynn, D. Lawson, M. Turmaine, S. S. Namini, L. Chakrabarti, A. P. McMahon, K. R. Jessen, and R. Mirsky. 1999. 'Schwann cell-derived Desert hedgehog controls the development of peripheral nerve sheaths', *Neuron*, 23: 713-24.

Pellegatta, M., A. De Arcangelis, A. D'Urso, A. Nodari, D. Zambroni, M. Ghidinelli, V. Matafora, C. Williamson, E. Georges-Labouesse, J. Kreidberg, U. Mayer, K. K. McKee, P. D. Yurchenco, A. Quattrini, L. Wrabetz, and M. L. Feltri. 2013. 'alpha6beta1 and alpha7beta1 integrins are required in Schwann cells to sort axons', *J Neurosci*, 33: 17995-8007.

Pereira, J. A., R. Baumann, C. Norrmen, C. Somandin, M. Miehe, C. Jacob, T. Luhmann, H. Hall-Bozic, N. Mantei, D. Meijer, and U. Suter. 2010. 'Dicer in Schwann cells is required for myelination and axonal integrity', *J Neurosci*, 30: 6763-75.

Pereira, Jorge A., Yves Benninger, Reto Baumann, Ana Filipa Gonçalves, Murat Özçelik, Tina Thurnherr, Nicolas Tricaud, Dies Meijer, Reinhard Fässler, Ueli Suter, and João B. Relvas. 2009. 'Integrin-linked kinase is required for radial sorting of axons and Schwann cell remyelination in the peripheral nervous system', *J Cell Biol*, 185: 147-61.

Perlin, J. R., M. E. Lush, W. Z. Stephens, T. Piotrowski, and W. S. Talbot. 2011. 'Neuronal Neuregulin 1 type III directs Schwann cell migration', *Development*, 138: 4639-48.

Poliak, S., and E. Peles. 2003. 'The local differentiation of myelinated axons at nodes of Ranvier', *Nat Rev Neurosci*, 4: 968-80.

Pollard, Thomas D., Laurent Blanchoin, and R. Dyche Mullins. 2001. 'Actin dynamics', *Journal of Cell Science*, 114: 3.

Raeymaekers, P., V. Timmerman, E. Nelis, P. De Jonghe, J. E. Hoogendijk, F. Baas, D. F. Barker, J. J. Martin, M. De Visser, P. A. Bolhuis, and et al. 1991. 'Duplication in chromosome 17p11.2 in Charcot-Marie-Tooth neuropathy type 1a (CMT 1a). The HMSN Collaborative Research Group', *Neuromuscul Disord*, 1: 93-7.

Ramesh, Vijaya. 2004. 'Merlin and the ERM proteins in Schwann cells, neurons and growth cones', *Nature Reviews Neuroscience*, 5: 462.

Rasband, M. N., and E. Peles. 2015. 'The Nodes of Ranvier: Molecular Assembly and Maintenance', *Cold Spring Harb Perspect Biol*, 8: a020495.

Rasband, Matthew N., and Wendy B. Macklin. 2012. 'Chapter 10 - Myelin Structure and Biochemistry.' in Scott T. Brady, George J. Siegel, R. Wayne Albers and Donald L. Price (eds.), *Basic Neurochemistry (Eighth Edition)* (Academic Press: New York).

Rasi, K., M. Hurskainen, M. Kallio, S. Staven, R. Sormunen, A. M. Heape, R. L. Avila, D. Kirschner, A. Muona, U. Tolonen, H. Tanila, P. Huhtala, R. Soininen, and T. Pihlajaniemi. 2010. 'Lack of collagen XV impairs peripheral nerve maturation and, when combined with laminin-411 deficiency, leads to basement membrane abnormalities and sensorimotor dysfunction', *J Neurosci*, 30: 14490-501.

Readhead, Carol, and Leroy Hood. 1990. 'The dysmyelinating mouse mutations shiverer (shi) and myelin deficient (shimld)', *Behavior Genetics*, 20: 213-34.

Reilly, M. M., S. M. Murphy, and M. Laura. 2011. 'Charcot-Marie-Tooth disease', *J Peripher Nerv Syst*, 16: 1-14.

Ridley, Anne J. 2006. 'Rho GTPases and actin dynamics in membrane protrusions and vesicle trafficking', *Trends in Cell Biology*, 16: 522-29.

Riento, K., R. M. Guasch, R. Garg, B. Jin, and A. J. Ridley. 2003. 'RhoE binds to ROCK I and inhibits downstream signaling', *Mol Cell Biol*, 23: 4219-29.

Riento, K., N. Totty, P. Villalonga, R. Garg, R. Guasch, and A. J. Ridley. 2005. 'RhoE function is regulated by ROCK I-mediated phosphorylation', *Embo j*, 24: 1170-80.

Roach, A., N. Takahashi, D. Pravtcheva, F. Ruddle, and L. Hood. 1985. 'Chromosomal mapping of mouse myelin basic protein gene and structure and transcription of the partially deleted gene in shiverer mutant mice', *Cell*, 42: 149-55.

Rossor, A. M., J. M. Polke, H. Houlden, and M. M. Reilly. 2013. 'Clinical implications of genetic advances in Charcot-Marie-Tooth disease', *Nat Rev Neurol*, 9: 562-71.

Saher, G., B. Brugger, C. Lappe-Siefke, W. Mobius, R. Tozawa, M. C. Wehr, F. Wieland, S. Ishibashi, and K. A. Nave. 2005. 'High cholesterol level is essential for myelin membrane growth', *Nat Neurosci*, 8: 468-75.

Saporta, M. A., I. Katona, R. A. Lewis, S. Masse, M. E. Shy, and J. Li. 2009. 'Shortened internodal length of dermal myelinated nerve fibres in Charcot-Marie-Tooth disease type 1A', *Brain*, 132: 3263-73.

Schindelin, Johannes, Ignacio Arganda-Carreras, Erwin Frise, Verena Kaynig, Mark Longair, Tobias Pietzsch, Stephan Preibisch, Curtis Rueden, Stephan Saalfeld, Benjamin Schmid, Jean-Yves Tinevez, Daniel James White, Volker Hartenstein,

Kevin Eliceiri, Pavel Tomancak, and Albert Cardona. 2012. 'Fiji: an open-source platform for biological-image analysis', *Nature Methods*, 9: 676.

Schmidt, A., and A. Hall. 2002. 'Guanine nucleotide exchange factors for Rho GTPases: turning on the switch', *Genes Dev*, 16: 1587-609.

Shah, Nirao M., Mark A. Marchionni, Indu Isaacs, Paul Stroobant, and David J. Anderson. 1994. 'Glial growth factor restricts mammalian neural crest stem cells to a glial fate', *Cell*, 77: 349-60.

Shao, J., W. J. Welch, N. A. Diprospero, and M. I. Diamond. 2008. 'Phosphorylation of profilin by ROCK1 regulates polyglutamine aggregation', *Mol Cell Biol*, 28: 5196-208.

Shen, Y. J., M. E. DeBellard, J. L. Salzer, J. Roder, and M. T. Filbin. 1998. 'Myelin-associated glycoprotein in myelin and expressed by Schwann cells inhibits axonal regeneration and branching', *Mol Cell Neurosci*, 12: 79-91.

Small, J., K. Rottner, P. Hahne, and K. I. Anderson. 1999. 'Visualising the actin cytoskeleton', *Microsc Res Tech*, 47: 3-17.

Sparrow, N., M. E. Manetti, M. Bott, T. Fabianac, A. Petrilli, M. L. Bates, M. B. Bunge, S. Lambert, and C. Fernandez-Valle. 2012. 'The actin-severing protein cofilin is downstream of neuregulin signaling and is essential for Schwann cell myelination', *J Neurosci*, 32: 5284-97.

Spiering, Désirée, and Louis Hodgson. 2011. 'Dynamics of the Rho-family small GTPases in actin regulation and motility', *Cell Adhesion & Migration*, 5: 170-80.

Stoll, G., and H. W. Muller. 1999. 'Nerve injury, axonal degeneration and neural regeneration: basic insights', *Brain Pathol*, 9: 313-25.

Susuki, Keiichiro, and Matthew N. Rasband. 2008. 'Molecular mechanisms of node of Ranvier formation', *Current opinion in cell biology*, 20: 616-23.

Takenawa, T., and S. Suetsugu. 2007. 'The WASP-WAVE protein network: connecting the membrane to the cytoskeleton', *Nat Rev Mol Cell Biol*, 8: 37-48.

Taveggia, C. 2016. 'Schwann cells-axon interaction in myelination', *Curr Opin Neurobiol*, 39: 24-9.

Taveggia, C., G. Zanazzi, A. Petrylak, H. Yano, J. Rosenbluth, S. Einheber, X. Xu, R. M. Esper, J. A. Loeb, P. Shrager, M. V. Chao, D. L. Falls, L. Role, and J. L. Salzer. 2005. 'Neuregulin-1 type III determines the ensheathment fate of axons', *Neuron*, 47: 681-94.

Terashima, T., H. Yasuda, M. Terada, S. Kogawa, K. Maeda, M. Haneda, A. Kashiwagi, and R. Kikkawa. 2001. 'Expression of Rho-family GTPases (Rac, cdc42, RhoA) and their association with p-21 activated kinase in adult rat peripheral nerve', *J Neurochem*, 77: 986-93.

Theveneau, Eric, and Roberto Mayor. 2012. 'Neural crest delamination and migration: From epithelium-to-mesenchyme transition to collective cell migration', *Developmental Biology*, 366: 34-54.

Topilko, P., S. Schneider-Maunoury, G. Levi, A. Baron-Van Evercooren, A. B. Chennoufi, T. Seitanidou, C. Babinet, and P. Charnay. 1994. 'Krox-20 controls myelination in the peripheral nervous system', *Nature*, 371: 796-9.

Tortora, G.J., and B. Derrickson. 2016. *Principles of Anatomy and Physiology* (J. Wiley).

Trapp, Bruce D., and Grahame J. Kidd. 2004. 'Chapter 1 - Structure of the Myelinated Axon.' in Robert A. Lazzarini, John W. Griffin, Hans Lassman, Klaus-Armin Nave, Robert Miller and Bruce D. Trapp (eds.), *Myelin Biology and Disorders* (Academic Press: San Diego).

Wakamatsu, Y., T.M. Maynard, and J.A. Weston. 2000. 'Fate determination of neural crest cells by NOTCH-mediated lateral inhibition and asymmetrical cell division during gangliogenesis', *Development*, 127: 2811-21.

Wallquist, W., S. Plantman, S. Thams, J. Thyboll, J. Kortesmaa, J. Lannergren, A. Domogatskaya, S. O. Ogren, M. Risling, H. Hammarberg, K. Tryggvason, and S. Cullheim. 2005. 'Impeded interaction between Schwann cells and axons in the absence of laminin alpha4', *J Neurosci*, 25: 3692-700.

Webster, Henry deF, John R. Martin, and Maureen F. O'Connell. 1973. 'The relationships between interphase Schwann cells and axons before myelination: A quantitative electron microscopic study', *Developmental Biology*, 32: 401-16.

Wen, J., C. Qian, M. Pan, X. Wang, Y. Li, Y. Lu, Z. Zhou, Q. Yan, L. Li, Z. Liu, W. Wu, and J. Guo. 2017. 'Lentivirus-Mediated RNA Interference Targeting RhoA Slacks the Migration, Proliferation, and Myelin Formation of Schwann Cells', *Mol Neurobiol*, 54: 1229-39.

Wen, J., D. Tan, L. Li, X. Wang, M. Pan, and J. Guo. 2018. 'RhoA regulates Schwann cell differentiation through JNK pathway', *Exp Neurol*, 308: 26-34.

Wennerberg, Krister, Marie-Annick Forget, Shawn M. Ellerbroek, William T. Arthur, Keith Burridge, Jeffrey Settleman, Channing J. Der, and Steen H. Hansen. 2003. 'Rnd Proteins Function as RhoA Antagonists by Activating p190 RhoGAP', *Current Biology*, 13: 1106-15.

Weston, J. A. 1963. 'A radioautographic analysis of the migration and localization of trunk neural crest cells in the chick', *Dev Biol*, 6: 279-310.

Wheeler, Ann P., and Anne J. Ridley. 2004. 'Why three Rho proteins? RhoA, RhoB, RhoC, and cell motility', *Exp Cell Res*, 301: 43-49.

Witke, Walter. 2004. 'The role of profilin complexes in cell motility and other cellular processes', *Trends in Cell Biology*, 14: 461-69.

Wolpowitz, D., T. B. Mason, P. Dietrich, M. Mendelsohn, D. A. Talmage, and L. W. Role. 2000. 'Cysteine-rich domain isoforms of the neuregulin-1 gene are required for maintenance of peripheral synapses', *Neuron*, 25: 79-91.

Woodhoo, Ashwin, Maria B. Duran Alonso, Anna Droggiti, Mark Turmaine, Maurizio D'Antonio, David B. Parkinson, Daniel K. Wilton, Raya Al-Shawi, Paul Simons, Jie Shen, Francois Guillemot, Freddy Radtke, Dies Meijer, M. Laura Feltri, Lawrence Wrabetz, Rhona Mirsky, and Kristján R. Jessen. 2009. 'Notch controls embryonic Schwann cell differentiation, postnatal myelination and adult plasticity', *Nature Neuroscience*, 12: 839.

Wu, Yuwen, Lasse Dissing-Olesen, Brian A. MacVicar, and Beth Stevens. 2015. 'Microglia: Dynamic Mediators of Synapse Development and Plasticity', *Trends in immunology*, 36: 605-13.

Wulf, E., A. Deboben, F. A. Bautz, H. Faulstich, and T. Wieland. 1979. 'Fluorescent phallotoxin, a tool for the visualization of cellular actin', *Proc Natl Acad Sci U S A*, 76: 4498-502.

Yang, D., J. Bierman, Y. S. Tarumi, Y. P. Zhong, R. Rangwala, T. M. Proctor, Y. Miyagoe-Suzuki, S. Takeda, J. H. Miner, L. S. Sherman, B. G. Gold, and B. L. Patton. 2005. 'Coordinate control of axon defasciculation and myelination by laminin-2 and -8', *J Cell Biol*, 168: 655-66.

Zalc, B., D. Goujet, and D. Colman. 2008. 'The origin of the myelination program in vertebrates', *Current Biology*, 18: R511-R12.